



**Politecnico
di Torino**

Master's Degree in Mechanical Engineering

Department of Mechanical and Aerospace Engineering

Master's Degree Thesis

**Local Marine Renewable Energy Resource Assessment
via bias correction of climate re-analysis datasets**

Supervisors:

Prof. MARKEL PENALBA RETES

Prof. GIORGI GIUSEPPE

Candidate:
GUO CHAO

Sep 2022

content

.....	1
Abstract	4
Introduction.....	5
1. Data collection.....	8
1.1 Literature review of different data sources	8
1.2 Data classification.....	9
1.2.1 Buoy Measurements	9
1.2.2 ERA5 data	10
2. Initial resource assessment via statistical characterisation	11
2.1 Overall wave resource characterisation.....	11
2.1.1 Overall resource	12
2.2 Overall Wind resource characterisation.....	16
2.2.1 Average resource.....	16
2.3 post-processing data samples for every decade:	18
3. Bias Correction.....	20
3.1 Literature review	20
3.2 Classification of bias correction techniques.....	21
3.3 Modelling of Bias Correction techniques	23
3.4 data validation.....	23
3.5. Methodology	24
3.5.1 dataset validation	24
4. Results	27
4.1 Result of Delta method.....	27
4.1.1 Wave data	27
4.1.2 Wind data	28
4.2 Result of EQM (The empirical quantile mapping method) method.....	30
4.3 Result of EGQM (empirical Gumbel quantile mapping method) method.....	38
4.4 Bias correction in a different location	44
4.4.1 Cabo Begur (east of Spain)	44
4.4.2 Cabo Silleiro (west of Spain).....	51

4.4.3 Gulf Cadiz (south of Spain)	57
4.5 Summary of results for four locations.....	63
5. Conclusion and future work	64
Acknowledge	65
Reference	66

Abstract

This study focus on the assessment of climate simulation variables by exploiting different bias correction methods and analysis the comparison of different bias corrected simulation. Because measured models need to generate high resolution input data, global and regional climate models are often distorted and have poor resolution. The purpose of this study is to find an accurate bias correction approach for climate variables prediction which are used to estimate the potential of renewable energy in a local area. Three different bias correction methods are analyzed, one of them is simply to correct based on mean values of previous data while others are based on the choice of different quantiles. In order to ensure the accuracy of the study, an important assumption is that the statistical properties of the present climate bias are maintained in the future, which can guarantee the experimental results are useful in future climate predictions. The observation data are obtained using buoy measurement positioned in special locations and the original simulation data is simulated in ERA5 (the fifth generation ECMWF atmospheric reanalysis of the global climate). The main variables that are considered are H_s (significant wave height), T_p (peak period) and U_w (wind speed), which are corrected using three common bias corrections: Delta method, The Empirical Quantile Mapping method (EQM) and the Empirical Gumbel Quantile Mapping method (EGQM). These three bias correction (BC) methods are used to correct original simulation data, making it as close to the observation as possible, and finally the most suitable method would be selected to correct the simulation data in the future, for which on the study of Spanish coast, is the EQM.

Key words: offshore renewable energy; resource assessment; climate re-analysis models, buoy data; bias correction;

Introduction

Due to the warning signals of climate change to human beings, countries all over the world have been thinking about how to reduce carbon emission and save energy. To reduce dependence on fossil energy, many countries start using nuclear energy, but the continuous occurrence of nuclear facility accidents has increased the doubts about the safe use of nuclear energy. Therefore, safe and clean renewable energy becomes the trend in the future development, especially ocean renewable energy (ocean energy), which refers to the renewable energy contained in the ocean due to the special background environment of the ocean, mainly including offshore wind energy (fixed and floating), tidal energy, wave energy, temperature difference energy, etc. But according to the report "Oceans Offer Solutions to Climate Change" published by the High level Panel on a Sustainable Ocean Economy in 2019, only 0.3% of global electricity generation comes from marine renewable energy currently. And the world's marine renewable energy reserves have reached more than 75 billion kilowatts, which means that, assuming the utilization efficiency of marine energy is 10%, the renewable energy contained in the ocean can fully meet the future electricity demand of human society.

In recent years, the establishment of offshore energy farms has provided new ideas for the use of ocean energy. In order to reasonably utilize these renewable energy sources, it is first necessary to calculate and predict the future energy production capacity of the region. This project aims to compare the past observation data and simulation data based on global-scale reanalysis, and apply different Bias Correction (BC) methods. The objective is to improve the simulation data to approximate the observed values, and find the most suitable (closest fitted data) correction method to predict future climate trends and changes in climate parameters in the region.

Global Climate Models (GCMs) has been the original simulation for hydro meteorological research, and it is the fundamental for assessing the impacts of climate change at all levels. However, for real climate studies, GCMs are rarely used directly because systematic errors exist in this original simulation, commonly due to simplified physical modes, poor spatial resolution and thermodynamic processes or other unrecognized knowledge about climate parameters. Errors in GCM simulations relative to historical observations can be large (*Ramirez-Villegas et al. 2013*). Hence, the use of a BC method is necessary in order to get a precise data that are

significantly closing the gap between the original simulation and observation point. Bias Correction is also used to overcome critical bias in climate models and various methods have been developed. It is important that for all methods, the quality of the observed data determines the quality of bias correction. To have a good observational dataset, long-term observed data sets are necessary.

Several BC methods are applied in this study, the first and simplest approach to reduce errors, commonly named as the “Delta” method (Hay et al., 2000), which is applied by reducing the mean difference between observation and simulation from simulation datasets. After that, different bias correction methods have been applied, from time averaged corrections to higher distribution moments corrections (Piani et al., 2010). A more precise simulation calibration has been created by using linear/nonlinear regression methods (e.g., Hay and Clark et al., 2003; von Storch and Zwiers et al., 1999; Miguez et al., 2011), quantiles analysis methods (e.g., empirical quantile mapping; Déqué, 2007; Boé et al., 2007; Amengual et al., 2012), among others, like fitted histogram equalization (Piani et al., 2010) and gamma-gamma transformation (Sharma et al., 2007). The most advanced quantile mapping methods are often used to better fit the variance of the simulated distribution to the observed variance. (Teutschbein and Seibert et al., 2012), performing a quantile-based transformation of distributions (Panofsky and Brier et al., 1968). BC are employed in many climate research that include hydrology and meteorology parameters, like winds, temperature and precipitation (Hemer et al., 2012; Applequist, 2012; Terink et al., 2009), local wave and tidal climate research (e.g., Charles et al., 2012) are also included.

For climate researches, few studies on the application of BC techniques to dynamic global wave climate projections are available in the scientific literature. This study implement several BC methods, applied to H_s (wave height), T_p (peak period) and U_w (wind speed) in different positions around Spain, eg. Gulf of Biscay, Galicia, Gulf of Cadiz and Cape of Creus. The observation data that we used are obtained from buoy measurement positioned in special locations provided by the ‘Spanish Oceanography Agency Puertos del Estado’, and the original simulation data are given by ERA5, which is the fifth generation ECMWF (European Centre for Medium-Range Weather Forecasts) atmospheric reanalysis of the global climate. Reanalysis combines observation model data all over the world into a globally complete and consistent dataset. ERA5 replaces its predecessor-- the ERA-Interim reanalysis.

After collecting all datasets, next step is post-processing with following rules:

- 1, interpolating dataset in one hour: the observation data in Bilbao Vizcaya are obtained every three hours, to get the datasets in every hour, linear interpolating method is used for both time data and observation data;
- 2, ignoring missing data (in the observation data with time interval greater than 7 days) and meaningless data (observation data that does not be recorded and using 99.99 in files) for each parameter and each year;
- 3, combine observation and simulation into one data file, observation and simulation data must have same time period and same number.

The data will be compared and displayed through statistical metrics (mean, root mean square deviation (RMSD), Pearson correlation coefficient (PC) and standard deviation (δ_y)) illustrated via Taylor diagrams, which are usually used to evaluate the accuracy of the model.

The results of final study show that the simple Delta method (changing the simulation mean) can improve the performance of original simulation, but the results still provide poor accuracies. Because the simple Delta correction changes the average of the overall data, there is not much improvement for extreme data. In comparison, EQM and EGQM have a significant improvement on the original data. EQM is applied by 99 linear divided quantiles, and for EGQM, due to the selection of different quantiles higher than 99%, the extreme data has a good improvement.

The reminder of the work is as follows: In Section 1 of the thesis, different datasets are presented. The performance and comparison of observation data and original simulation data are assessment in Section 2. For Section 3, several BC methods are used to correct the simulation data, and the results and conclusion will be displayed in Sections 4 and 5, respectively.

1. Data collection

1.1 Literature review of different data sources

Observed and simulated climate can be thought of as a sample of a time-dependent multivariate probability distribution—multivariate in space, in time and between different climatic variables.

In Fig.1.1 (Douglas Maraun et al., 2016)

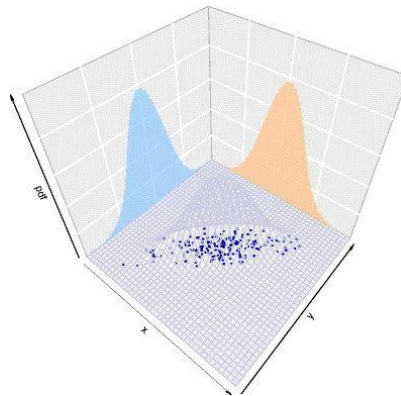


Fig.1.1 two-dimensional distribution (time and space)

Global Climate Model (GCM) is a mathematical formulation of processes related to the climate system, including the formation of radiative, wind power transport, clouds formation, water evaporation and heat transport by ocean currents. Climate models are useful to predict future weather conditions. The obtained knowledge can lead to policy decisions related to climate change. One of the benefits of GCM is its ability to operate multiple simulation researches using different greenhouse gas emission scenarios. The downside of GCM is that it cannot solve spatial features smaller than 50 miles by 50 miles.

Regional Climate Model (RCM) is a numerical weather prediction model enforced by oceanic conditions determined from atmospheric circulation models (GCMs) or observational data (Reanalysis) Simulate processes and land areas in the atmosphere. It should also be considered high-resolution topographic data, land-sea contrasts, surface characteristics, and other components of the Earth-system. Because RCM only covers a limited area, the limits of these values must be clearly stated which are called boundary conditions. These boundary conditions are Results through thicker GCM or new analysis.

Global Climate Models are large models that simulate the behavior of atmospheric circulation models with a total resolution of about 100-250 km. Therefore, a downscaling technique must be used to achieve results at a finer resolution of 25-50 km. RCM model is the most commonly

used technology. The highest resolution RCM and complex physical processes are able to reproduce and project detailed climate data that cannot be captured by GCM.

Global Wave hindcasts (GOW2) provides information on wave weather conditions over long periods of time. This improves our understanding of climate variability, long-term and extreme trends. This information is useful for coastal researches and can also be used directly for regional and local downscaling boundary conditions. GOW2 is used to obtain wave climate simulations over a reference historical period. It has multiple grids, being the parent grid 0.5° (latitude) x 0.5° (longitude). The wave spectral domain varies from 0.0373 Hz to 0.7159 Hz with 32 logarithmically spaced frequencies and 24 directions (15° resolution). In contrast to altimeter and buoy data, the validation of GOW2 performs better agreement between the coastal and offshore datasets, same condition happens for the high ranking quantiles.

1.2 Data classification

For datasets analysis in this study, in order to make reasonable predictions, two kinds of data have been chosen and processed:

- 1, Buoy Measurements (Observation data): Ocean buoys measure many meteorological variables, such as wave height, peak period, wave direction, wind speed and direction, air and water temperature, and barometric pressure.
- 2, ERA5 data (Original Simulation data): 'simulation is taking a large amount of data and using it to simulate or mirror real-world conditions to either predict a future instance, determine the best course of action or validate a model.' [Drew Robb May 21, 2021]

1.2.1 Buoy Measurements

Instead of using the approaches above, valid climate observation datasets can also be downloaded through 'puertos del estado' (www.puertos.es/es-es/oceanografia/Paginas/portus.aspx), which is a State-owned company responsible for the management of state-owned ports of Spain.

In this study, 4 different observation sites around Spain were selected, namely Cabo Begur in the east, Cabo Silleiro in the west, Golf Cadiz in the south and Bilbao Vizcaya in the north, details of geographic coordinates are shown in the Table 1.1:

Buoy site	longitude	latitude
Cabo Begur	3.65°E	41.90°N
Cabo Silleiro	9.43°W	42.12°N
Golf Cadizin	6.96°W	36.49°N
Bilbao Vizcaya	3.69°W	40.42°N

Table1.1.buoy-measurement locations coordinate

The parameters selected to apply BC are H_s (wave height), T_p (peak period) and U_w (wind speed). Apart from the missing data, all parameters are recorded every three hours in 20th Century of Bilbao Vizcaya from 1990, while from 2000 to 2022 of Bilbao Vizcaya, Cabo Begur, Cabo Silleiro and Golf Cadizin, data are logged hourly.

1.2.2 ERA5 data

Original simulation data are obtained in ERA5. ERA5 --the fifth-generation of ECMWF(European Centre for Medium-Range Weather Forecasts) that are processed to analysis of global weather and climate over the past forty to seventy years. Current dataset is available start from 1959 to present. ERA5 provides hourly estimates for a large number of atmospheric, ocean-wave and land-surface quantities. Data has been re-gridded to a regular grid of 0.25 degrees for the reanalysis and 0.5 degrees for the uncertainty estimate (0.5 and 1 degree respectively for ocean waves) (ERA5 hourly data on pressure levels from 1959 to present.)

Taking the H_s (wave height) data of 'Bilbao Vizcaya' as an example, in order to compare and analyze it with data obtained from the observation, we selected the time period from 1990 to 2020, around 160,000 data samples. The comparison of original simulation and observation data in whole time period are displayed on Fig.1.2, where red line represents the buoy measurement data and blue line is the data from ERA5.

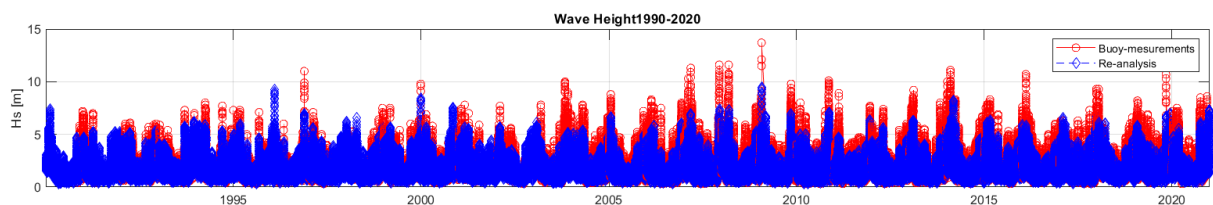


Fig.1.2 observation and original simulation data sample of H_s between 1990 and 2020

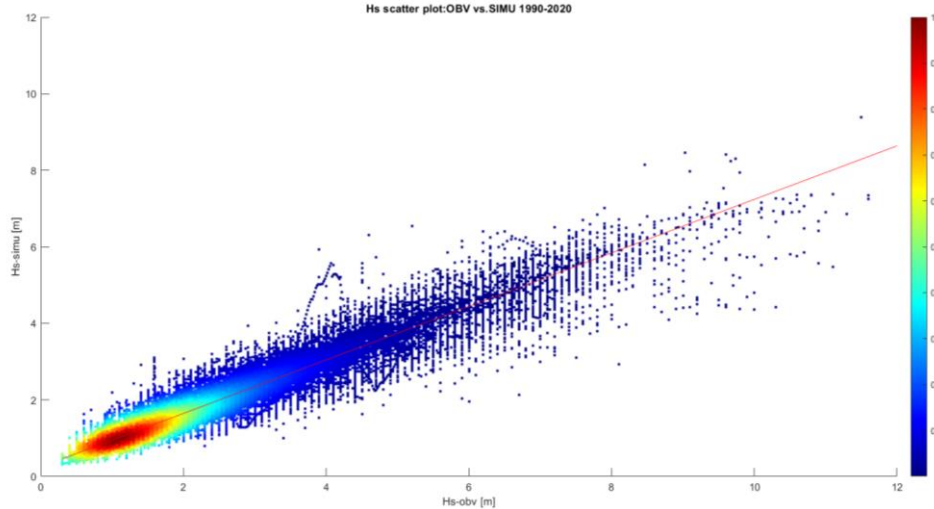


Fig.1.3 scatter density plot of H_s (1990-2020)

Scatter density plot (Fig.1.3) introduces the data density, using dots to represent values for observation and original simulation. The color bar on the right indicates the ratio of the number of points to the total number of points in the area. The closer the color to red, the higher the number of points in that area. Where x-axis is the dataset of observation and y-axis represents simulation data. From Fig.1.3, most of H_s wave height observation data are between 0m and 2m, which has scatter density around 1, same tendency happened for simulation, which has scatter density closer to 1.

2. Initial resource assessment via statistical characterisation

To better analyse and understand the tendency of raw datasets, wave resources and wind resources are estimated respectively.

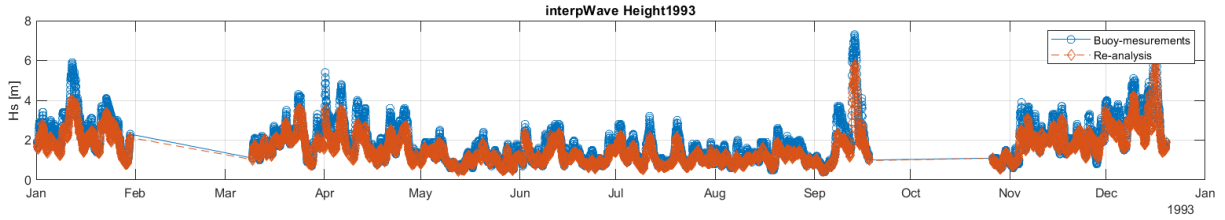
2.1 Overall wave resource characterisation

Three main variables will be studied in this thesis, two of them related to wave resources--- H_s (wave height) and T_p (peak period). These two parameters have significant impacts on the production of ocean energy, the higher the wave height, the more wave energy would be generated. Having the same wavelength, a wave with higher height will produce more power when it falls back to sea level than a wave of lesser height. Energy per square meter is proportional to the square of the wave height (H_s): $E \propto H_s^2$. T_p (peak period) is defined as the time interval between two adjacent peaks, which represent how long two adjoining waves produce maximum energy.

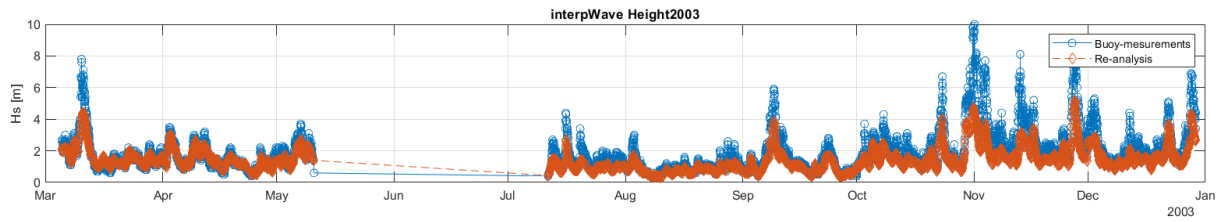
2.1.1 Overall resource

Taking samples of Bilbao Vizcaya as an example, 4 separate years (1993, 2003, 2013 and 2020) were chosen for comparison. In order to get a clear vision between observation and simulation data, raw observation and simulation data after interpolating and post-processing are used. H_s and T_p are shown on Fig. 2.1 and Fig. 2.3:

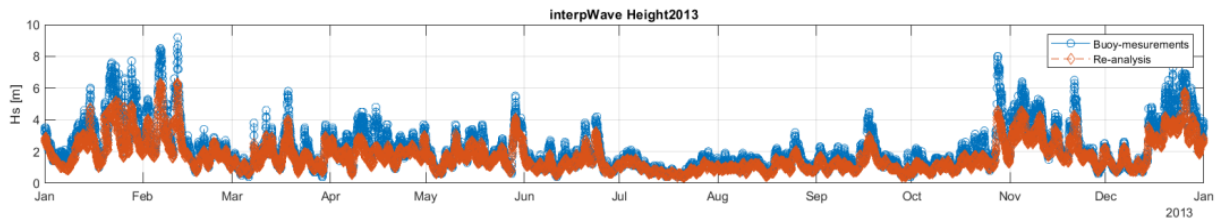
H_s (Bilbao Vizcaya):



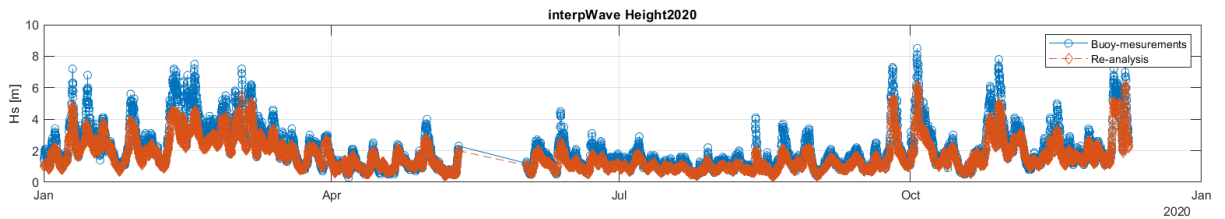
Hs 1993 (Raw data of observation and simulation after interpolating and post-processing)



Hs 2003 (Raw data of observation and simulation after interpolating and post-processing)



Hs 2013 (Raw data of observation and simulation after interpolating and post-processing)



Hs 2020 (Raw data of observation and simulation after interpolating and post-processing)

Fig2.1 H_s Raw data of Bilbao Vizcaya after interpolating and post-processing

In Fig2.1, the blue line introduces the observation data (buoy-measurement) and red line is the original simulation data. From the figures above, wave height has less fluctuations in this region from April to September, most of the data are lower than 4m for both observation and simulation. While from October to March of the following year, wave height changes more clearly, and extreme values always occur during this time period for all samples. Reading from figures, the highest wave height is around 10m. This is of course related to the local climatic environment and ocean current conditions. The unique oceanic climate along the coast and the North Atlantic circulation combine together generate hydrological features in this sea area.

The density of the data and its corresponding value can be visually represented by the scatter density plot (Fig. 2.2):

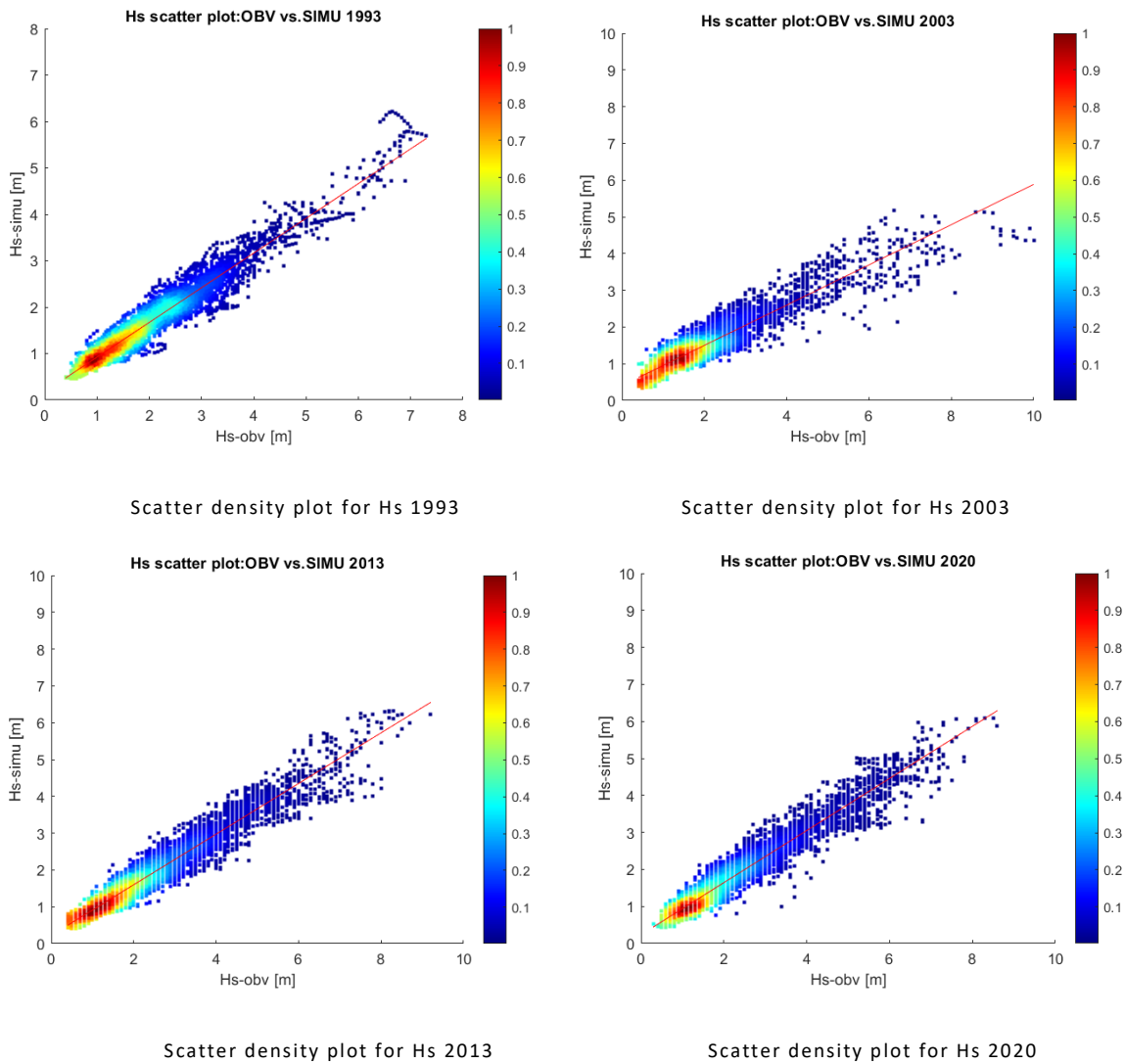
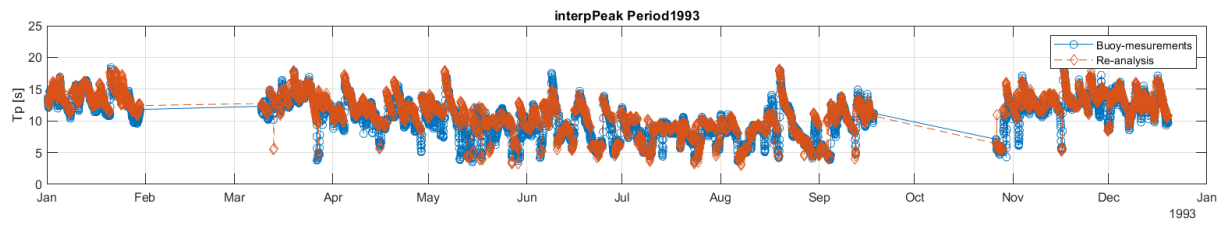


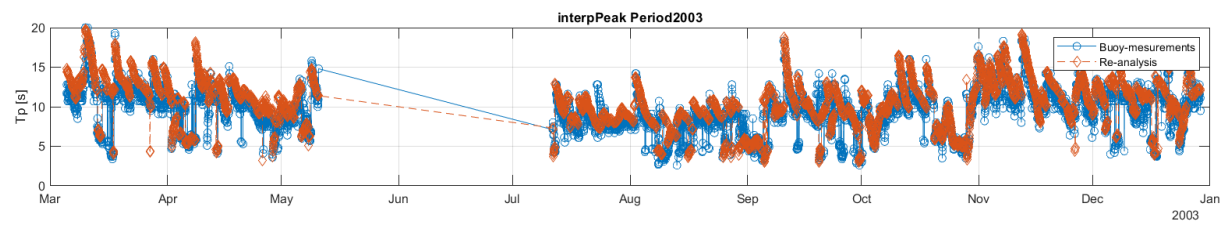
Fig. 2.2 Scatter density plot for H_s (Bilbao Vizcaya)

Where for 1993, the vast majority of observation values are around 0.919m, the vast majority of simulations are equal to 0.875m, and their scatter density is 0.996. Situations changes for 2003, the largest number of observation value of it is 1.3m and largest number of simulation value is 1.139m, scatter density is 0.995. As for 2013, these three values are 1.2m for observation, 0.969m for simulation and 0.987(scatter density); for 2020, they are 1.2m (observation), 1.017m (simulation) and 0.993 (scatter density), respectively.

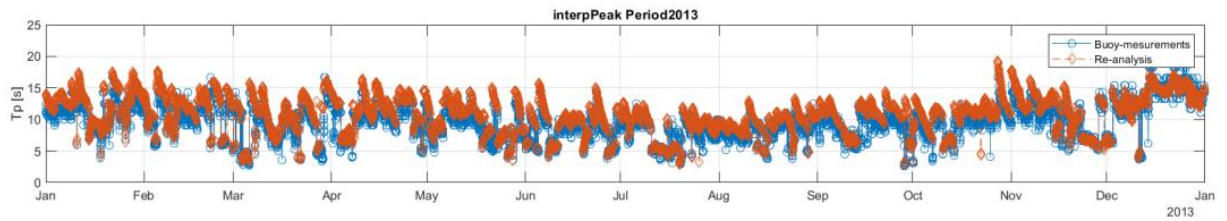
T_p (Bilbao Vizcaya):



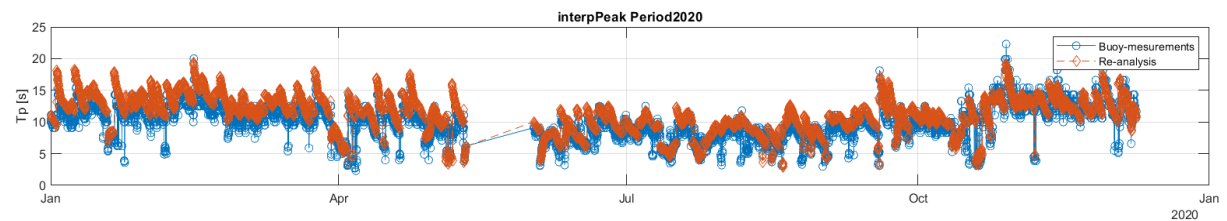
T_p 1993 (Raw data of observation and simulation after interpolating and post-processing)



T_p 2003 (Raw data of observation and simulation after interpolating and post-processing)



T_p 2013 (Raw data of observation and simulation after interpolating and post-processing)



T_p 2020 (Raw data of observation and simulation after interpolating and post-processing)

Fig. 2.3 T_p Raw data of Bilbao Vizcaya after interpolating and post-processing

For T_p (peak period) of the observation and simulation data, sample trend and maximum point are not as clear as what shown on H_s . But differences can also be found between time period A (from May to October) and B (October to April of the following year). The transition of samples in time period A is relatively gradual and does not produce a sudden rise or reduction. However, data in time period B are relatively different, the ups and downs of the points are obvious and maximum point always occurs in this area. Specific data can be obtained by scatter density plot (Fig.2.4).

Scatter density plot for T_p (Bilbao Vizcaya):

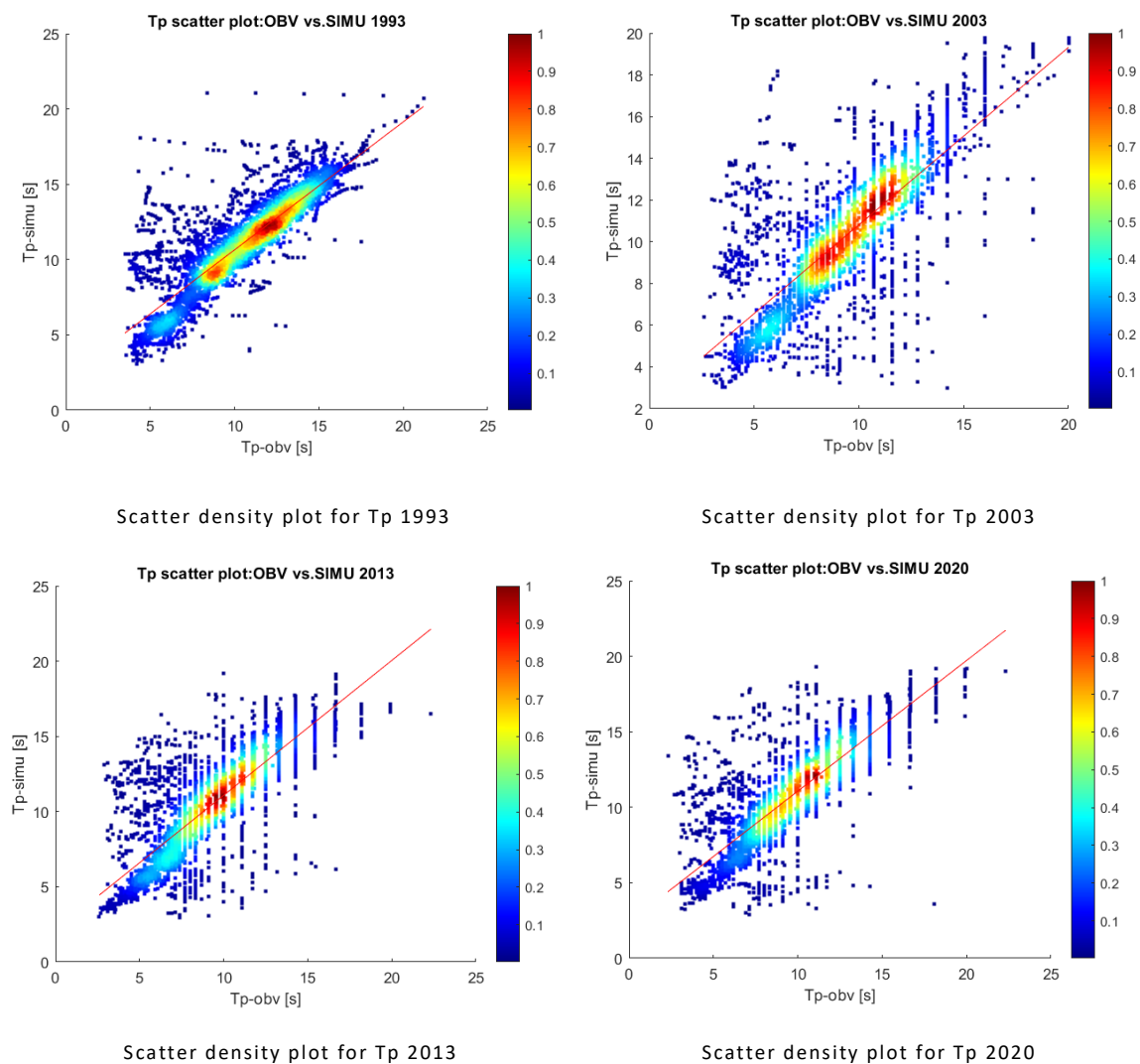


Fig. 2.4 Scatter density plot for T_p (Bilbao Vizcaya)

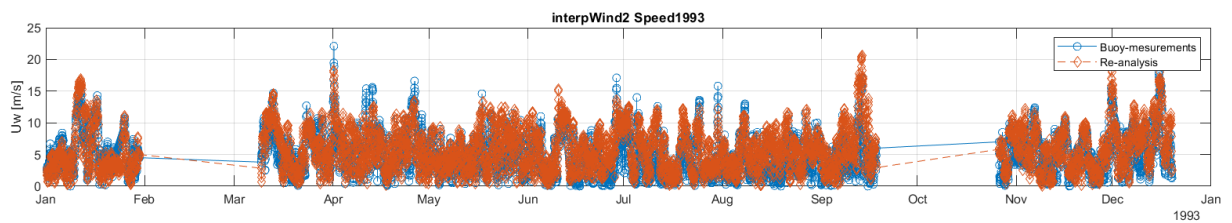
For 1993 and 2003, the vast majority of observation values for both figures are between 10s and 15s, the vast majority of simulation values are between 12s and 14s. Almost same situations happened for 2013 and 2020. For extreme values, its number is higher than 20s and lower than 22s for 1993, but for the other three years, extreme values are less than 20s.

2.2 Overall Wind resource characterisation

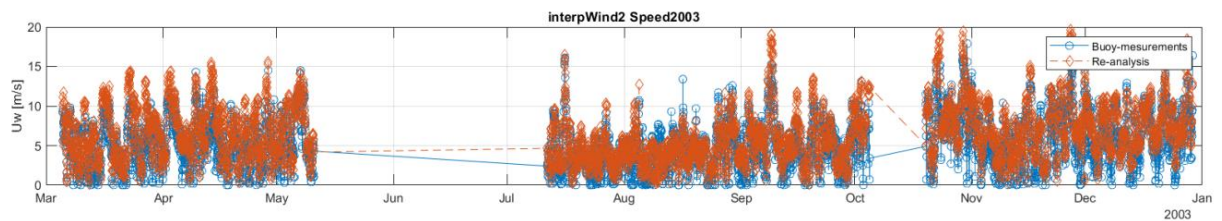
Several parameters affect the energy generation related to wind resource, and in this study, the most significant variable has been chosen—wind speed. Wind speed largely determines the amount of electricity generated. The greater the wind speed and the longer the duration of the wind, the greater the wave energy will be produced.

2.2.1 Average resource

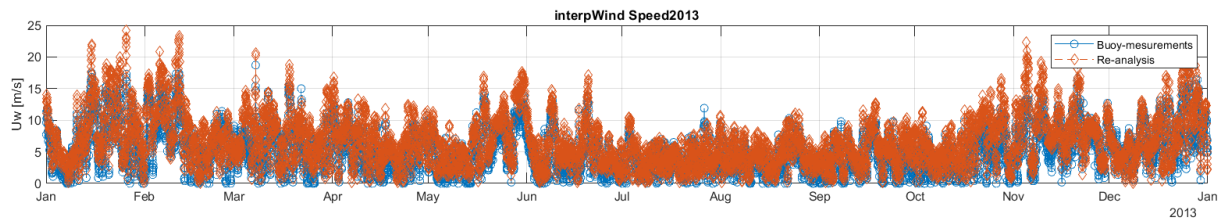
Same location and same year are selected as it displayed for wave resources, but for U_w (wind speed), instead of using the original observation and simulation data, post-processing data would be more clearly to reflect the trend of sample, which are shown in (Fig.2. 5):



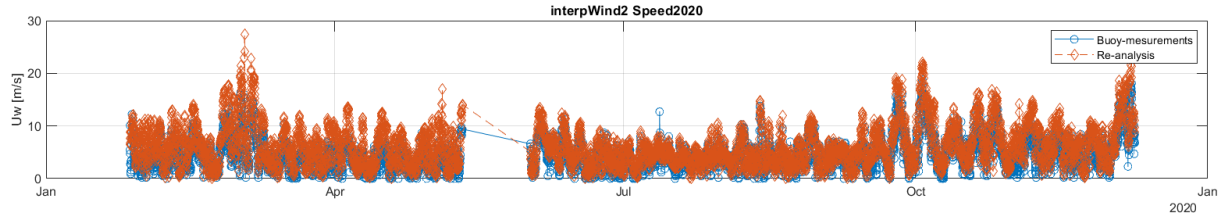
Uw 1993 Raw data of observation and simulation after interpolating and post-processing



Uw 2003 Raw data of observation and simulation after interpolating and post-processing



Uw 2013 Raw data of observation and simulation after interpolating and post-processing



Uw 2020 Raw data of observation and simulation after interpolating and post-processing

Fig.2.5 Uw Raw data of Bilbao Vizcaya after interpolating and post-processing

2.2.1.1 Overall resource

Unlike H_s and T_p , there is no obvious difference in U_w , but the sample fluctuation in summer and autumn is slightly smaller than that in spring and winter.

Scatter density plot for U_w (Bilbao Vizcaya):

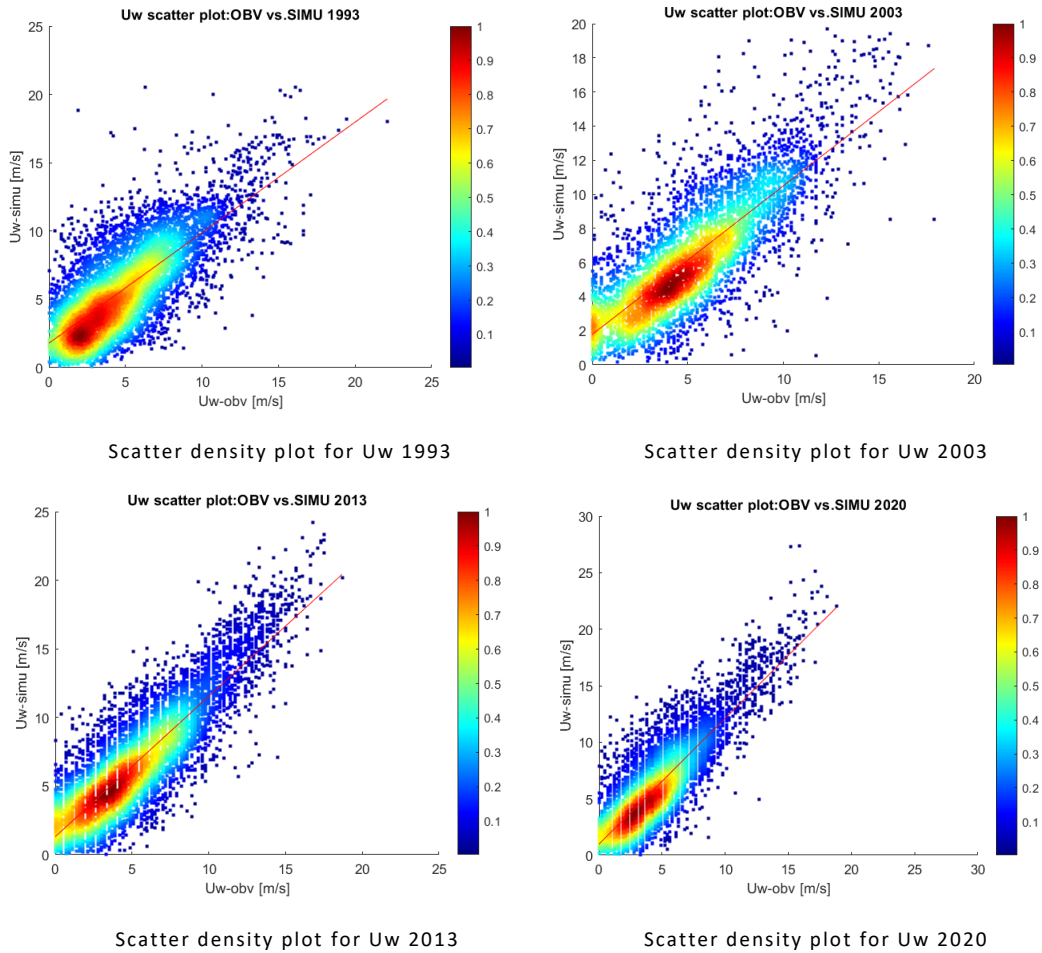


Fig. 2.6 Scatter density plot for U_w

Like what it shown on sample data, same situation also displayed in scatter density plot. From the figure above, observation samples focuses on range between 0 and 10 m/s, simulation data focuses on range 0 and 10 m/s. Most samples located in this large area, which also means the fluctuation is not so evident during the whole period.

2.3 post-processing data samples for every decade:

Data samples (during 1990—2000, 2001—2010 and 2011—2020):

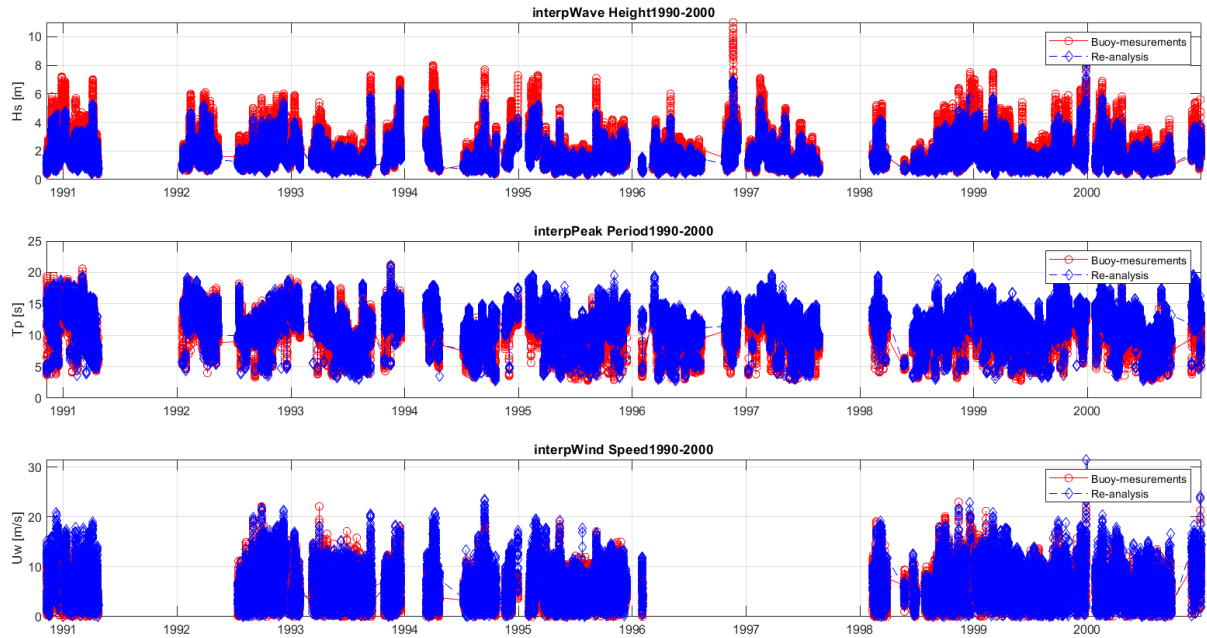


Fig. 2.7 data sample 1990—2000

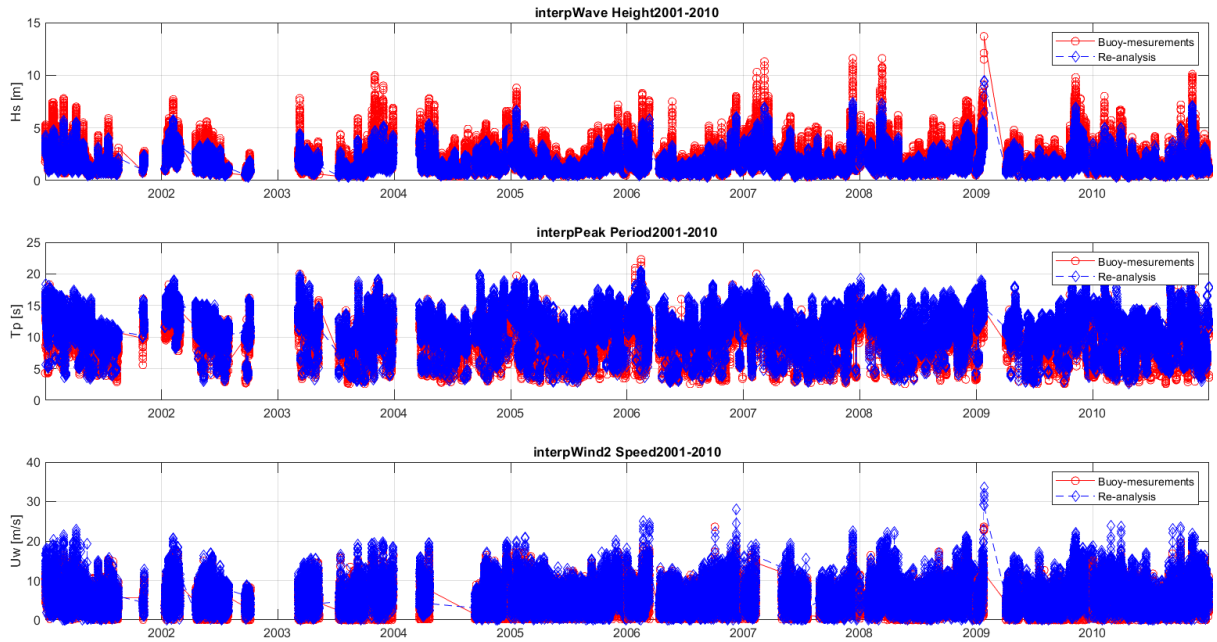


Fig. 2.8 data sample 2001—2010

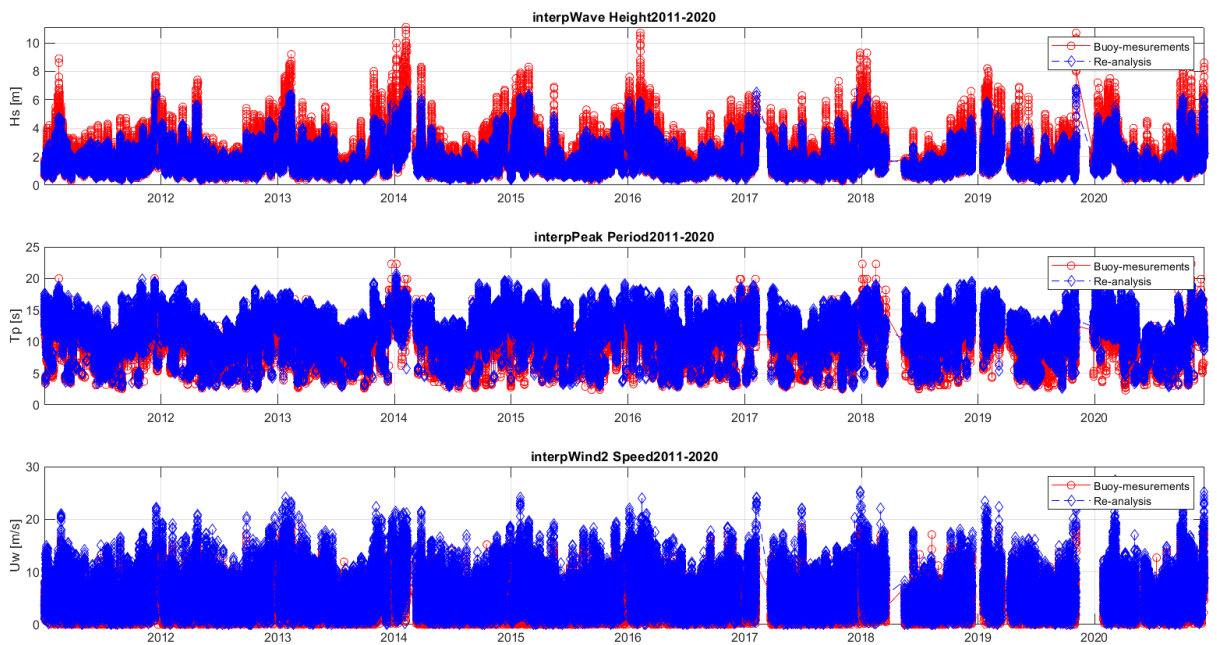


Fig. 2.9 data sample 2011—2020

These figures above are the comparison of observation and simulation datasets after data post-processing. The original datasets for both observation and simulation cannot be used directly not only because they choose different time interval, but missing data and incorrect recordings are also exist. Therefore, one hour time interval has been chosen during the whole period, by

linearly interpolating approaches changing simulation from three hour interval to one hour, removing missing data that has time period over one week and ignoring meaningless data. At the same time, if the number of missing data higher than 50 percent of the total data number for each year, it says invalid and we will not take this data into account.

These three figures are post-processing data for observation and original simulation, ignoring missing data and meaningless data, which will be the input data for BC.

In the 20th century, weather data records were not very accurate, especially wind speed records, there were many missing and invalid data, and in some years useful data were even less than 50%, such as 1992 and 1997. After that, the data quality has gradually improved, and it has been relatively complete in recent years, indicating that people are paying more attention to weather changes and renewable energy sources.

3. Bias Correction

3.1 Literature review

The wave and wind source forecast statistics that climate models provide during the control period often do not match observations for the same period. There are systematic errors in the results of both global and regional climate models (GCM, RCM). For instance, climate models often have lower wave height simulation and often underestimate the extreme values of it. Bias in climate simulation may be caused by a number of reasons. Errors due to this condition may affect simulated results for future time. Therefore, using inaccurate results in climate impact often produces unrealistic results. In order to solve these errors in climate models, a number of bias correction methods have been developed. The bias correction approach has been created to improve the suitability of climate model simulations to observations during the control period, it is also used to improve the reliability of climate model results for future time. As with all methods, it is significant to realise that the quality of the observed data dominates the quality of bias correction result. So, a good set of observations is the prerequisite for good bias correction. If extreme values need to be corrected, then long-term effective data collection is essential.

Bias correction is the process of scaling climate model outputs to account for their systematic errors, in order to improve their fitting to observations (Teutschbein, et al., 2010).

3.2 Classification of bias correction techniques

1, Delta method:

The simplest BC, proposed by (Hay et al., 2000), is the Delta method, also called “perturbation method” (Themeßl et al., 2012; Fowler and Kilsby, 2007; Graham et al., 2007). This method is used to adjust the variable distribution of simulation data by adding each value the difference between the observation mean data and the simulation mean data that computed using (Eq. 1).

The approach is applied to each dataset at each value, defined as:

$$Hs_i^C = Hs_i^{simu} + (\overline{Hs^{obv}} - \overline{Hs^{simu}}) \quad i = 1, \dots, N \quad (\text{Eq. 1})$$

Where Hs_i^C is the H_s (wave height) after applying bias correction, Hs_i^{simu} is the original simulation that will be bias corrected, $\overline{Hs^{obv}}$ and $\overline{Hs^{simu}}$ are the mean values for observation and reference simulation samples, calculated for the choosing reference time period, and N is the length of the time period. Because Delta Correction method is operated for every single time point, errors from original simulations would be added to the corrected simulation datasets. Also, using Delta Correction to change means for original samples ignores extreme values that located in high quantiles, which is a disadvantage for this approach.

In this project, Delta bias correction method is used for H_s , T_p and U_w respectively, and the reference time period are separated into every decade (ie.1990-2000, 2001-2010, 2011-2020); every twenty years (ie.1990-2010, 2001-2020) and every thirty years (ie.1990-2020).

After statistical computation, which represented in Section 4.1, the PC (correction coefficient) and δ_y (standard deviation) between the original simulated data and corrected data are the same, while RMSD are different. Compared with original simulation, the RMSD for corrected simulations are reduced which means the corrected sample is closer to the observation data on Taylor diagram (in section 4.1.1 and 4.1.2). The statistical meaning of RMSD is to measure the error between real data and simulated data, smaller RMSD means smaller error between them, so the corrected simulation value using Delta method is better than the original one.

2, The empirical quantile mapping method (EQM)

Using statistical techniques to reduce systematic bias in numerical climate model simulations is an important tool in applied research. One of the common tools used to correct bias in climate

model simulations is EQM, mapping between simulations and observed cumulative distribution (CDF) functions based on data from historical periods. However, EQM is very simple and robust in some cases, which are known to have inherent problems, especially in correcting biases in future climate projections.

While comparing to Delta method, this is a more complex form of bias correction, where the simulated (empirical) cumulative distribution function ECDF is calibrated by supporting to each simulated ECDF interval a specific quantile correction (i.e., linearly divide simulation dataset 1st to 99th quantiles, adding to each single simulation dataset interval the difference between the inverse of observation ECDF and the inverse of simulation ECDF). The correction term is computed at each linearly spaced quantiles, as the inverse of observation ECDF minus the inverse of simulation, equations are as following (eg. use H_s as an example):

$$X(q_i) = ECDF^{obv^{-1}}(q_i) - ECDF^{simu^{-1}}(q_i), i = 1, \dots, n_q \text{ (Eq.2)}$$

$$H_s^C(q_i) = H_s^{simu}(q_i) + X(q_i), i = 1, \dots, n_q \text{ (Eq.3)}$$

Where H_s^{simu} and H_s^C are the original simulated datasets and datasets after bias correction respectively. The EQM method is purely empirical since no assumptions about the distributions are made (Wilcke et al., 2013), By correcting each quantile in particular, the EQM method accounts for different error characteristics of different quantiles, leading to a better BC than other methods (Wilcke et al., 2014; Themeßl et al., 2011).

3. The empirical Gumbel quantile mapping method (EGQM)

The EGQM method is a correction of a simulated empirical cumulative distribution function ECDF (Wilks et al., 1995), by adding corresponding correction terms to the data between adjacent and quantiles (pre-set). EGQM is an improved method of EQM, the only difference is that it uses the Standard Gumbel distribution (SGD; Gumbel et al., 1935) instead of the evenly distributed quantile as the correction term, it is therefore can better perform the correction of the upper-tailed distribution, which means a better correction for extreme values. For the operation of the EGQM approach, using the standard Gumbel distribution (SGD), choosing the number of quantiles to be 20 between the 1st quantile and the 99.999th quantile. Most of our quantiles are larger than 95th percentile, focusing on the correction of the extreme values,

where higher biases are usually found (Gil Lemos, et al., 2020), (On the need of bias correction methods for wave climate projections Gil Lemos), such as:

$$x_{qi} = q_{lo} + (i - 1) \frac{q_{up} - q_{lo}}{n_q}, i = 1, \dots, n_q$$

$$q_i = \exp[-\exp(-x_{qi})], i = 1, \dots, n_q \text{ Eq. (4)}$$

Where q_i is the quantiles computed from the SGD, $q_{lo} = 1$ and $q_{up} = 99.999$. The method was then implemented as in (Eq.(2) and Eq.(3)), by applying correction terms calculated as the difference between the inverse ECDFs of simulation and observation, at each quantile q_i (as in Eq. (4)), linearly interpolating between them.

3.3 Modelling of Bias Correction techniques

All numerical simulations and modeling work in this study are done through Matlab. In the Delta method, after preprocessing the observation and simulation data, the difference between the averages of the two samples in every five years and every ten years is selected as the correction term for Delta BC.

While EQM and EGQM are relatively complex. In EQM, 99 quantiles are selected linearly by the 'quantile' command, a matrix is constructed for each two adjacent quantiles, which contains all the values within this interval, and the data is rearranged into the corresponding matrix. In each matrix of the interval, the inverse cumulative distribution function operation is performed to obtain the corrected result. Compared with the linear selection of EQM, EGQM adopts the 'gumbel distribution' method in quantile selection, which selects extreme quantiles. The next calculation steps are the same with EQM method.

3.4 data validation

We analysis the differences between observation and simulation datasets from several ways of expression:

- 1, scatter plot between observation and simulation, also plot the fit line (like what we did above);
- 2, computing and comparing mean value, root mean square deviation (RMSD), Pearson correction coefficient (PC) and standard deviation (δ_y) for both datasets;

- 3, plotting Taylor diagram for every year, every five year, and every decade;
- 4, making distribution line for every year, every five year, and every decade.

In this section, in order to judge the agreement of the corrected results, some statistical parameters need to be calculated and statistical diagrams need to be drawn, the parameters are listed below and the most useful diagram would be the Taylor diagram.

3.5. Methodology

3.5.1 dataset validation

Dataset validation is essential to make sure that the simulated and observed datasets introduce the correct metocean conditions of a given location. To that end, the most relevant variables obtained from the buoy measurements (observation) and the re-analysis (original simulation) data are compared by means of statistical metrics for the time-period is very important. And in some cases, statistical parameters can quantitatively show the characteristics of the sample and the improvement of the overall data after correction. The statistical parameters used for data analysis and comparison are the Root Mean Square Deviation (RMSD), Pearson correlation coefficient (PC) is employed for the analysis of similarity and the Standard deviation (δ_y), equations of these three parameters are following (eg. using H_s as example, all the equations for T_p and U_w are the same):

- 1, Root Mean Square Deviation (RMSD), The RMSD represents the square root of the second sample moment of the differences between simulated values and observed values or the quadratic mean of these differences, The RMSD is very sensitive to the much large or small errors in a set of measurements, so it can reflect the precision of the measurement very well.

$$\text{RMSD}_{H_s} = \sqrt{\frac{\sum_{n=1}^N (\widehat{H}_s - H_{s_n})^2}{N}} \quad \text{Eq. (5)}$$

Where \widehat{H}_s is the variable obtained from the observation model, H_{s_n} is the simulation variable and N is the number of meaningful samples considered within the validation time period.

2, Pearson correlation coefficient (PC) is a linear correlation coefficient and it is the most commonly used correlation coefficient. It is used to reflect the degree of linear correlation between two variables X and Y. The value is between -1 and 1. The larger the absolute value, the stronger the correlation, the formula is:

$$PC = \frac{cov(\widehat{H}_s, H_s)}{\widehat{\delta}_y \delta_y} \text{ Eq. (6)}$$

Where $cov(\widehat{H}_s, H_s)$ is the covariance, $\widehat{\delta}_y$ and δ_y are the standard deviation for simulated and observed dataset respectively.

3, Standard deviation (δ_y) is defined as the square root of the arithmetic mean of the square of the difference between the standard value and its mean. It reflects the degree of dispersion among individuals within a group, which defined as:

$$\delta_y = \sqrt{\frac{1}{N} \sum_{n=1}^N (H_s - \mu_y)^2} \text{ Eq. (7)}$$

And μ_y represent the mean value of samples, which is a measure of central tendency of a finite set of numbers, defined as:

$$\mu_y = \frac{1}{N} \sum_{n=1}^N (H_{S_n}) \text{ Eq. (8)}$$

By using these statistical values, a Taylor diagram can be easily plotted that represent the similarity between simulation and observation, which also introduce the difference before and after bias correction method.

Taylor diagram was first proposed by Karl E. Taylor in 2001, mainly used to compare the ability of several meteorological models of simulation, which is simply a chart that can represent three indicators: standard deviation (δ_y), root mean square deviation (RMSD) and correlation coefficient (PC). It is more intuitive than a single RMSE and other horizontal and vertical coordinates.

It can centrally represent the relevant information of multiple models, and is an effective method widely used in model evaluation and testing in recent years. It can comprehensively display 3 different parameters on a two-dimensional map, the multi-mode simulation capability can be fully and clearly reflected.

For instance:

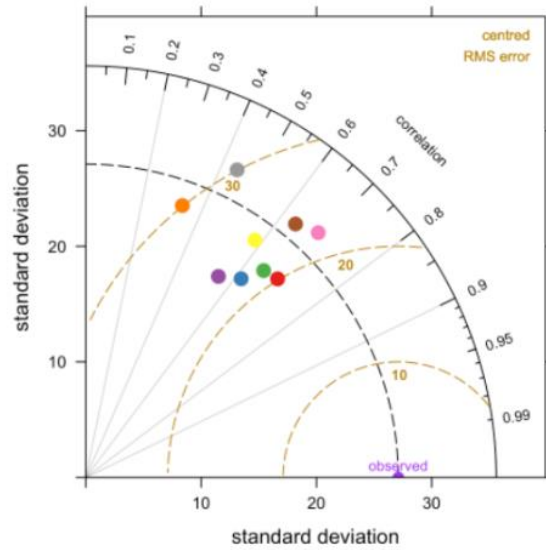


Fig.3.1 example of Taylor diagram

Fig.3.1 is an example of Taylor diagram, for the red point, its pattern correction is between 0.7 and 0.75, while the closer the coefficient is to 1, the better the correlation; the orange dash line indicates the RMSD value, so the centered RMSD is 20, the standard deviation is the distance between the red point and the origin, in this case around 20. The 'observed (purple)' is observation, the closer to the observed point, the more similar to the realistic, the better the correction part has been done. From the figure, red point is closest to observation, means it generally agrees best to the realistic.

4. Results

The results of corrected simulation using different BC will be shown below, which includes one Delta method, two EQM methods and one EGQM method.

4.1 Result of Delta method

To check the validation of Delta bias correction method, the simulation datasets are divided into several time-slices: present climate used to compute the BC (bias correction), different time periods and different time intervals can be used to find a better correction value. It includes 3 kinds of time intervals and 6 different time period: every decade (ie.1990-2000, 2001-2010, 2011-2020); every twenty years (ie.1990-2010, 2001-2020) and every thirty years (ie.1990-2020). The datasets during 2001-2020 are used as fundamental dataset to compare the validation of different time intervals.

4.1.1 Wave data

Wave data includes H_s (wave height) and T_p (peak period). The observation, original simulation datasets and simulation data after Delta BC correction through different years are integrated in the Table4.1 and Table4.2 below,

H_s	2001-2020 (fundamental)		Mean [m]	RMSD [m]	PC [-]	σ_y [m]
		Buoy	1.945	0.000	0.000	1.238
	Simu	1.598	0.564	0.965	0.891	
every decade	1990-2000(cor)	corrected	1.907	0.447	0.965	0.891
	2001-2010(cor)	corrected	1.939	0.446	0.965	0.891
	2011-2020(cor)	corrected	1.949	0.446	0.965	0.891
every 20 years	1990-2010(cor)	corrected	1.924	0.446	0.965	0.891
	2001-2020(cor)	corrected	1.945	0.446	0.965	0.891
every 30 years	1990-2020(cor)	corrected	1.934	0.446	0.965	0.891

Table4.1: H_s (wave height) for the validation of original simulation & corrected simulation model with respect to observation.

Where the statistical values are the last four columns (mean, RMSD, PC correction coefficient, standard deviation), the first two rows indicate the values of observation and original simulation, the rest of the rows are corrected values after Delta BC using different years correction terms.

The Pearson correction coefficient (PC) and standard deviation (δ_y) do not change after Delta BC and the values are 0.965 and 0.891 respectively. This is obvious because we add a correction term for each value and its means changes the same. While RMSD is the only parameter should

be considered and for H_s , it is almost the same, which means the degree of dispersion is not changed much when corrected with different years. Although corrected values show similar numbers, there is a high improvement compared with original simulation both for mean value and RMSD.

Because PC and δ_y do not change, the Taylor diagram is not so clear to tell the difference, so a bar plot (Fig.4.1 (a)) is enough:

T_p (peak period):

Same trend happened for T_p , the value of PC is 0.819 and δ_y is 2.911 that are the same for all simulation samples. Before correction, the mean value of original simulation is 10.842 that is larger than observed 9.665. This condition has been improved after BC, all of these 'Means' are closer to observation than before.

Tp			Tp(peak period)			
			Mean [s]	RMSD [s]	PC [-]	σ_y [s]
	2001-2020 (fundamental)	Buoy	9.655	0.000	0.000	2.606
		Simu	10.842	2.061	0.819	2.911
every decade	1990-2000(cor)	corrected	9.798	1.692	0.819	2.911
	2001-2010(cor)	corrected	9.683	1.686	0.819	2.911
	2011-2020(cor)	corrected	9.631	1.686	0.819	2.911
every 20 years	1990-2010(cor)	corrected	9.736	1.688	0.819	2.911
	2001-2020(cor)	corrected	9.655	1.686	0.819	2.911
every 30 years	1990-2020(cor)	corrected	9.696	1.686	0.819	2.911

Table 4.2: T_p (peak period) for the validation of original simulation & corrected simulation model with respect to observation.

Different values of 'RMSD' for T_p are in Fig.4.1 (b):

4.1.2 Wind data

U_w (wind speed) is the only wind data considered in this study, whose mean value of observation is 5.078 m/s and original simulation mean is 6.201m/s. From the table below, using the correction term from 2001-2020 works best, and the corrected data is closest to the observation, its mean value equal to 5.106m/s and RMSD is 1.935. Of course, all simulations of

U_w after Delta BC show better performance than before with same PC equal to 0.843 and same δ_y equal to 3.592.

Uw			Uw(wind speed)			
	2001-2020 (fundamental)		Mean [m/s]	RMSD [m/s]	PC [-]	σ_y [m/s]
		Buoy	5.078	0.000	0.000	3.031
every decade	1990-2000(cor)	corrected	5.716	2.037	0.843	3.592
	2001-2010(cor)	corrected	5.362	1.956	0.843	3.592
	2011-2020(cor)	corrected	4.849	1.948	0.843	3.592
every 20 years	1990-2010(cor)	corrected	5.539	1.989	0.843	3.592
	2001-2020(cor)	corrected	5.106	1.935	0.843	3.592
every 30 years	1990-2020(cor)	corrected	5.194	1.938	0.843	3.592

Table4.3: Uw (wind speed) for the validation of original simulation & corrected simulation model with respect to observation.

The situation of RMSD of U_w is as same as before, displayed on Fig.4.1 (c)

As showing in the above table, for each variable, PC (Pearson correction coefficient) and δ_y (standard deviation) are the same, RMSD is the parameter that only changed by using Delta bias correction. In this case, Taylor diagram is not a convenient approach to show the comparison, and a bar plot is easily to represent its difference:

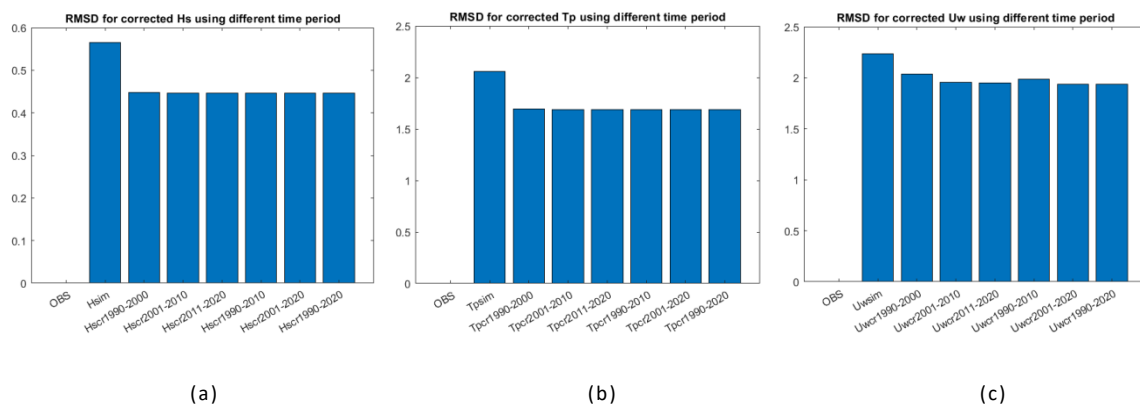


Fig. 4.1 RMSD for Hs Tp and Uw in different time period

Where 'OBS' is the observation data that set as '0', H_{sim} , Tp_{sim} , Uw_{sim} are the original simulated RMSD for H_s , T_p and U_w . $H_{s_{cr}}$, Tp_{cr} , Uw_{cr} are the corrected RMSD value. As can be seen in these three plots, all corrected RMSD are smaller than the original one so the Delta BC actually improve the simulation dataset, making it closer to the observation part.

For H_s , after using the above time intervals' correction, its minimum RMSD difference between original simulation and corrected simulation is 0.1173, the maximum difference is 0.1189, that does not change so much. Same situation happens for T_p and U_w : for T_p , minimum difference is 0.3696, maximum difference is 0.3757; for U_w , minimum difference is 0.2, maximum difference is 0.302.

4.2 Result of EQM (The empirical quantile mapping method) method

There are two approaches to use the EQM method:

- 1, using CDF in the whole dataset, correcting simulation bias without different intervals;
- 2, dividing the dataset using 99 quantiles, and implement CDF computing for each part separately. The result of EQM method to correct data is better than Delta method whenever using the first or the second method. While comparing the first approach, the corrected simulation that using 99 quantiles are closer to the observation, the example result of H_s , T_p and U_w are displayed below:

Hs			Hs(wave height)			
	1990-2020 (fundamental)		Mean [m]	RMSD [m]	PC [-]	σ_y [m]
			Buoy	1.937	0.000	0.000
		Simu	1.601	0.547	0.966	0.882
		2(using 99 quantiles)	1.937	0.083	0.997	1.218
		1(without 99 quantiles)	1.937	0.318	0.998	1.217

Table4.4 Statistical values compare 1 and 2 for Hs

Tp			Tp(peak period)			
	1990-2020 (fundamental)		Mean [s]	RMSD [s]	PC [-]	σ_y [s]
			Buoy	9.763	0.000	0.000
		Simu	10.909	2.019	0.823	2.888
		2(using 99 quantiles)	9.763	0.166	0.998	2.640
		1(without 99 quantiles)	9.763	1.568	0.999	2.637

Table4.5 Statistical values compare 1 and 2 for Tp

Uw			Uw(wind speed)			
	1990-2020 (fundamental)		Mean [m/s]	RMSD [m/s]	PC [-]	σ_y [m/s]
			Buoy	5.232	0.000	0.000
		Simu	6.201	2.222	0.832	3.598
		2(using 99 quantiles)	5.232	0.169	0.999	3.084
		1(without 99 quantiles)	5.232	1.795	0.998	3.083

Table4.6 Statistical values compare 1 and 2 for Uw

Where '2' represent statistical values for method using 99 quantiles and '1' includes values using CDF in the whole dataset. 'simu' is the original simulation value (without bias correction) and 'Buoy' for observation data.

By concluding from the table, the mean H_s value for observation is 1.937m, while for original simulation, it is 1.601m. After bias correction, mean value became 1.937m for both EQM methods, get very close to observation.

Same results happened for PC (Pearson correlation coefficient) and δ_y (standard deviation), the bias corrected simulation becomes more similar to observed value that are around 0.997 and 1.218 respectively. These parameters are almost the same by using the two EQM methods above.

While for RMSD, the RMSD for original simulation, bias corrected values using the '2' method and '1' method are 0.547m, 0.0833m and 0.3178m respectively. Although bias correction made RMSD better, the difference between '2' method and '1' method are large, and 0.0833m ('2' method) is smaller than 0.3178m ('1' method), which means '2' method performs better degree of dispersion than '1' method.

For T_p (peak period) and U_w (wind speed), same situations are displayed---mean, PC and δ_y show almost the same value for both EQM methods, while the differences between RMSD are large. And the RMSD for method '2' is smaller than using method '1', means two bias correction EQM methods made data more similar than original simulation and using 99 quantiles to do the CDF has better results than compute CDF on whole dataset.

Another interesting thing is to compare it with the Delta method, EQM has smaller RMSD, especially for method '2' (using 99 quantiles), and really good PC coefficient (around 1). The standard deviation of EQM method is closer to observation than original and Delta BC simulation, and the plot of sample data before and after BC are as follow in Fig.4.2.

Plot Fig.4.2 (a) is the sample data for observation, original simulation, corrected simulation using Delta, EQM method '1' and EQM method '2', Fig.4.2 (b) introduce the CDF for all datasets.

Because there are too many data samples in one plot, we can only see the general trend through Fig.4.2. Therefore, Fig.4.2 (a) has been zoomed in, in order to observe the specific

changes before and after correction and using different correction methods, results (general result chosen in average value area) has been displayed on Fig.4.3(a).

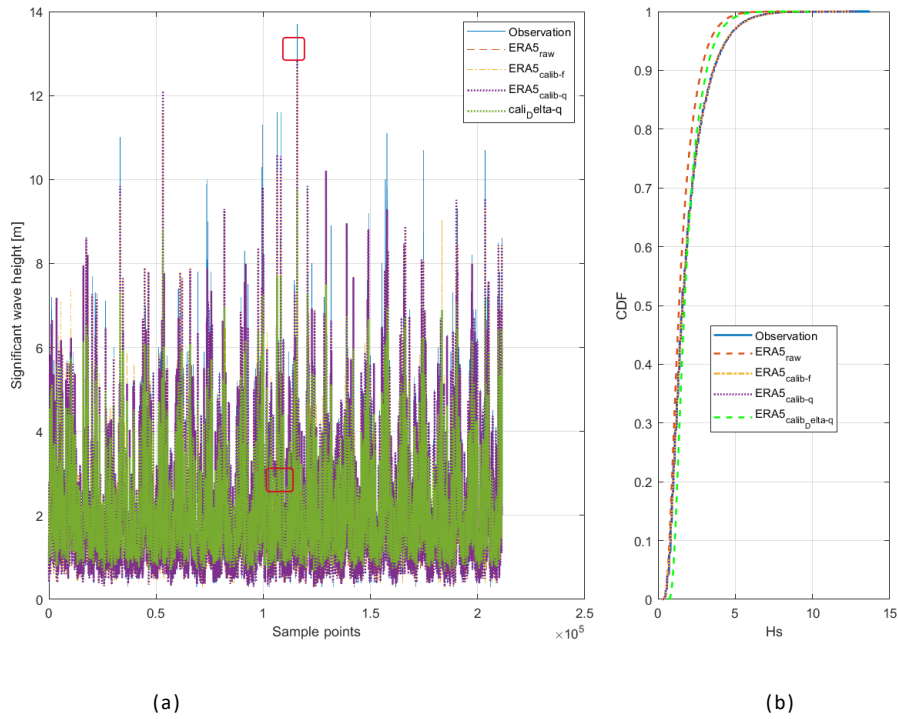


Fig.4.2 Hs data samples and CDF plot for DELTA and EQM method

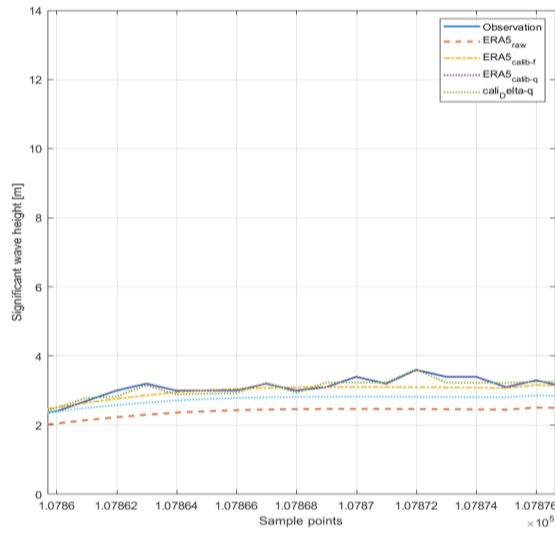


Fig.4.3 (a) zoomed in sample for average value

Where Fig.4.3(a) is the lower red circle on Fig.4.2 (a), which represent the average sample value of the whole H_s data. As for the zoomed in part of all samples, straight blue line represents the observation data, orange dash line is the original simulation, yellow line is corrected sample

using EQM method '1' (without 99 quantiles), the corrected data for EQM method '2' is shown in purple dash, and the green line displays Delta correction method.

Compared Delta correction method with original simulation, after Delta BC, the simulation samples has moved up and be significantly closing the gap between simulation and observation. EQM (using 99 quantiles) can not see clearly in this figure because it is almost overlap with the observation, which is by far the most suitable method. So a simple result can be concluded that the effect of correction for H_s is EQM (using 99 quantiles) > EQM (without 99 quantiles) > Delta method.

The EQM and Delta for T_p is shown below:

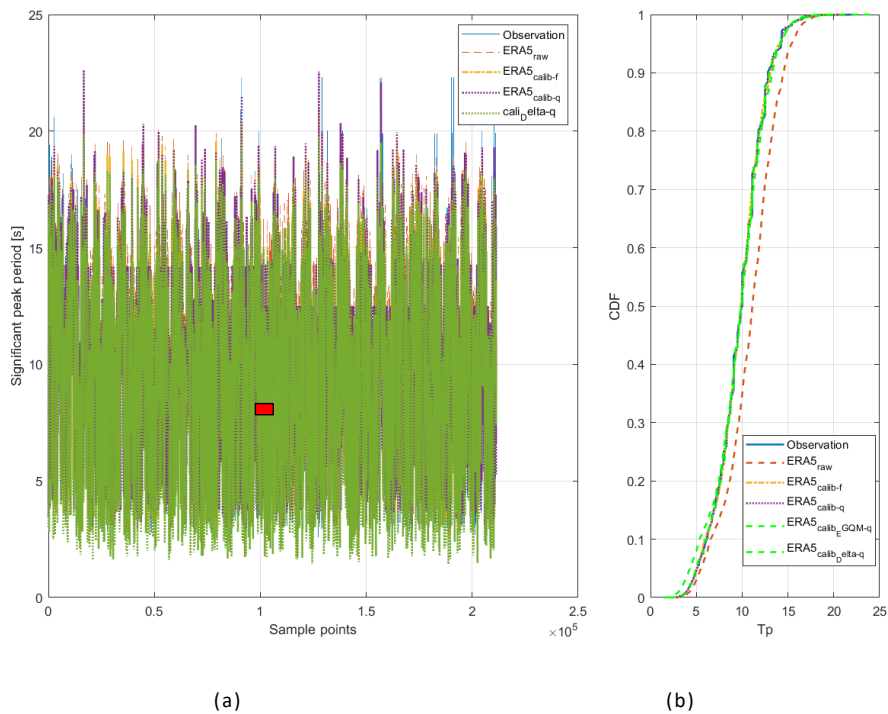


Fig.4.4 data samples and CDF plot for DELTA and EQM method(T_p)

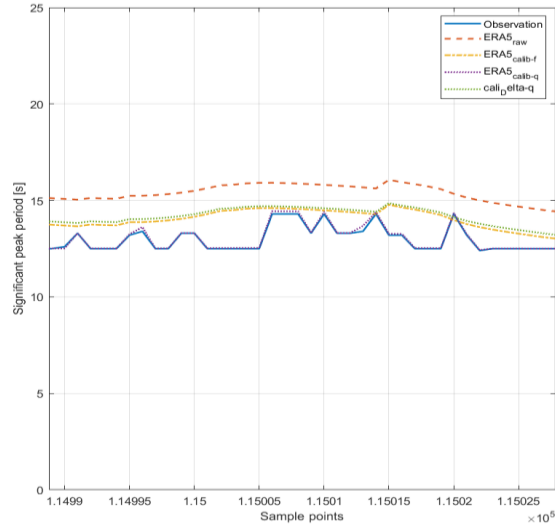


Fig4.5 zoomed in sample for average value

For T_p , Fig4.5 is the zoomed in area of red square in Fig.4.4(a), the original simulation is overestimated, while in some parts of the figure, Delta method fit better than the EQM (without 99 quantiles), and the EQM (using 99 quantiles) is always the most similar simulation to the observation.

The EQM and Delta for U_w is shown below:

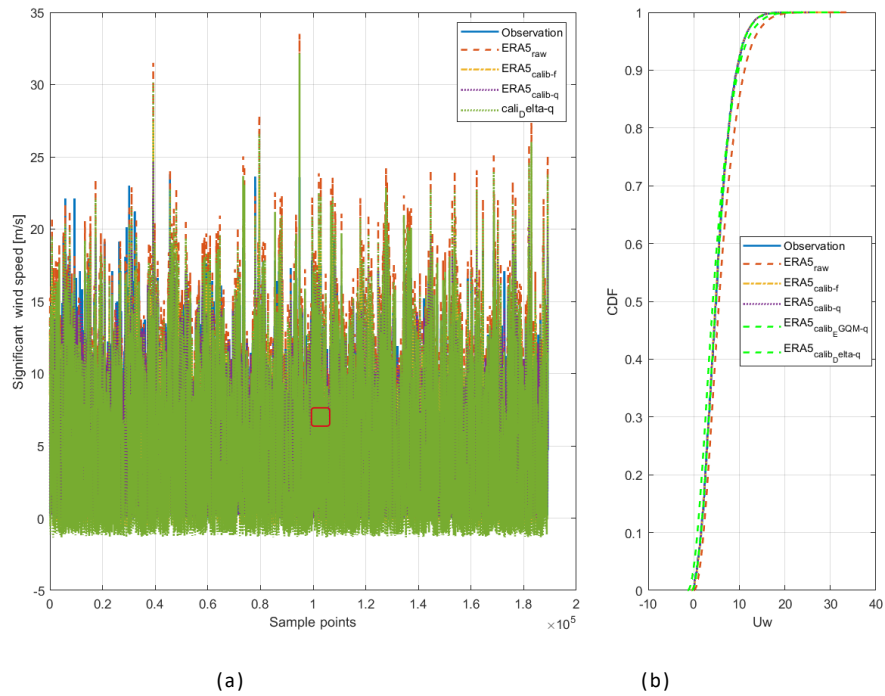


Fig.4.6 data samples and CDF plot for DELTA and EQM method (U_w)

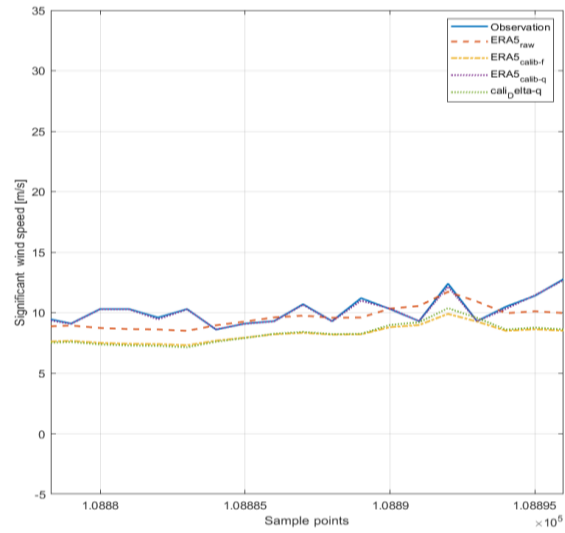


Fig4.7 zoomed in plot for data sample

For U_w , Fig4.7 is the zoomed in area of red square in Fig.4.6 (a), and same situation happened, original simulation is a little bit overestimated. For Delta and the EQM (without 99 quantiles), we can not see which one is better. And there is no doubt that EQM (using 99 quantiles) correction always suit the observation best.

Cause EQM (using 99 quantiles) fits the observation data very well, so the detail results of it are listed below:

EQM statistical values:

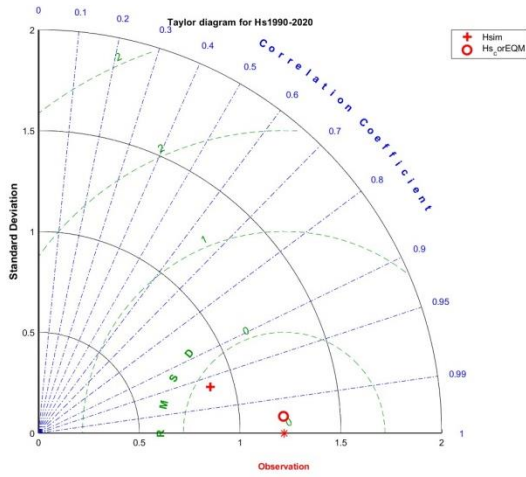


Fig.4.8 Taylor diagram for Hs (EQM)

Hs	Hs(wave height) EQM			
	Mean [m]	RMSD [m]	PC [-]	σy [m]
Buoy	1.937	0.000	0.000	1.218
Simu	1.601	0.547	0.966	0.882
EQMcor	1.937	0.083	0.998	1,218

Table4.7 statistical value for Hs (EQM)

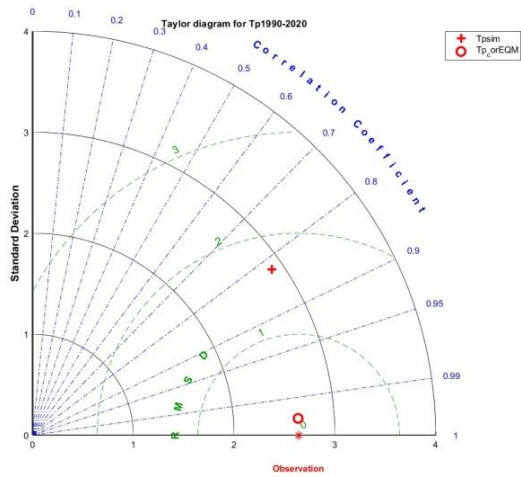


Fig.4.9 Taylor diagram for Tp (EQM)

Tp	Tp(peak period) EQM			
	Mean [s]	RMSD [s]	PC [-]	σy [s]
Buoy	9.763	0.000	0.000	2.641
Simu	10.909	2.019	0.823	2.888
EQMcor	9.763	0.166	0.998	2.640

Table4.8 statistical value for Tp (EQM)

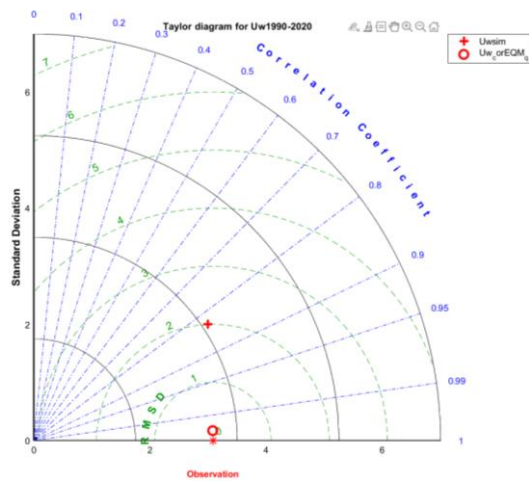


Fig.4.10 Taylor diagram for Uw (EQM)

Uw	Uw(wind speed) EQM			
	Mean [m/s]	RMSD [m/s]	PC [-]	σy [m/s]
Buoy	5.232	0.000	0.000	3.084
Simu	6.201	2.222	0.832	3.598
EQMcor	5.232	0.169	0.998	3.084s

Table4.9 statistical value for Uw (EQM)

Where in these charts, 'Buoy' is the observation data, 'Simu' includes the original simulation datasets and 'EQMcor' includes corrected datasets after EQM method (using 99 quantiles). And in Taylor diagram, '*' is the observation point, '+' represent the original simulation and 'o' is the bias corrected point using EQM method. As for original simulation dataset, comparing with H_s and U_w , T_p is the best, U_w shows the worst situation, because its 'Simu' point is farthest to its 'Obv' point.

In the H_s chart, the difference of mean value between 'buoy' and 'simu' is 0.336m, RMSD for original simulation is 0.547, correction coefficient (PC) is 0.966 and standard deviation is 1.218. While all these parameters change a lot after EQM bias correction, and the mean value of EQM correction is same with observation that is 1.937m, the difference between corrected data and observation is 0 that is true for both EQM approaches. They also have same standard deviation--1.218m. In contrast to 'Simu', RMSD, mean value and standard deviation of EQM corrected improve significantly, made it more similar to observation part, this can also be seen in Taylor diagram. The improving tendency for T_p and U_w are the same, moving the simulation point close to observation.

As for T_p , its observation data has mean value as 9.763s and standard deviation is 2.641, while these two values are 10.909s and 2.888 for original simulation. After EQM (using 99 quantiles), there is a higher improvement, 'mean' and ' δ_y ' are the same with observation, also with small RMSD (0.166) and much higher correction coefficient (0.998). A good correction is directly shown on Taylor diagram of Fig.4.9. Similar tendency can also be found on U_w that has higher PC (0.998) and low RSMD (0.169) and a higher quantity in contrast to the original simulation.

Although EQM BC shows good performance for most of the data, its correction effect on extreme data (which is the upper red square of Fig.4.3,) is not obvious, as shown in the Fig.4.3 (b) below:

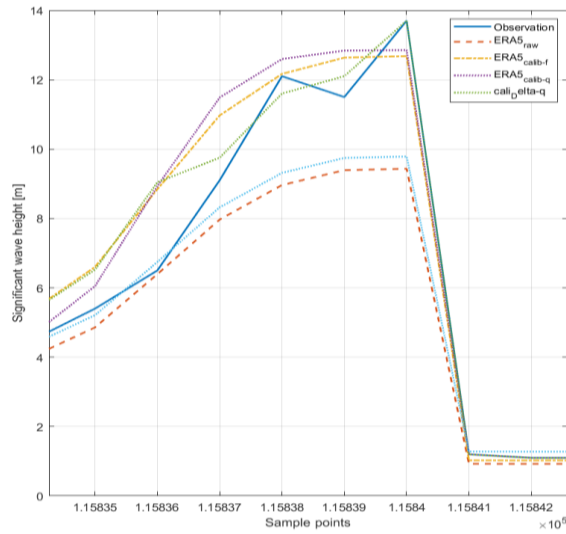


Fig.4.3(b) extreme sample for data sample above

The purple dash line (EQM) does not fit the blue line (observation) very well. In order to solve this problem, the EGQM method has been studied in the next part.

4.3 Result of EGQM (empirical Gumbel quantile mapping method) method

The EGQM method is usually useful to correct samples which have significant extreme values. Its steps are what we discussed in the section 3 before. As for the EQM method, there is a simple conclusion that using EQM (using 99 quantiles) fits observation best, so in this part, the comparison between EQM (using 99 quantiles) and EGQM will be presented.

For H_s , its statistical parameters and Taylor diagram are displayed below:

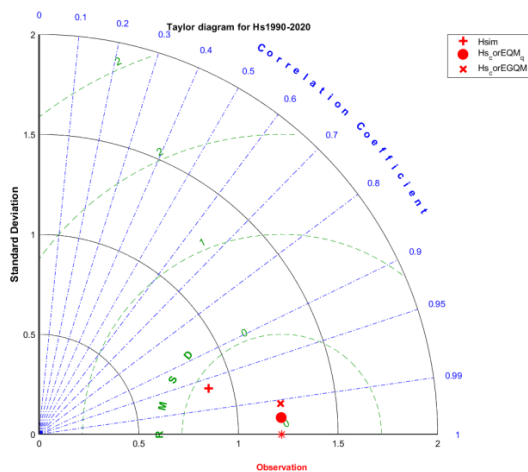


Fig4.11 Taylor diagram for Hs (EGQM)

Hs	Hs(wave height) EGQM				
		Mean [m]	RMSD [m]	PC [-]	σ_y [m]
Buoy		1.937	0.000	0.000	1.218
Simu		1.601	0.547	0.966	0.882
EQMcor		1.937	0.083	0.998	1,218
EGQMcor		1.938	0.154	0.992	1.221

Table4.10 statistical value for Hs (EGQM)

Where 'EGQMcor' refers to variable after using EGQM BC method, and the meaning of the other parameters is the same as before. There is no doubt that EGQM method improves quality of the original simulation data making it closer to the observation. Comparing its results with EQM, the mean value of EQM is 1.937, and it is 1.938 in EGQM, no noticeable difference, same situation happened for PC and standard deviation, which are 0.998, 1.218 for EQM and 0.992, 1,221 for EGQM. The main change comes from RMSD, where samples using EGQM is around two times higher than EQM, so the dispersion degree of EGQM with observation is higher than EQM with observation. In Taylor diagram, 'x' represents the sample corrected by EGQM, and same trend can be seen clearly, with the other two parameters are almost the same, RMSD is the only variance.

For T_p , its statistical parameters and Taylor diagram are displayed below:

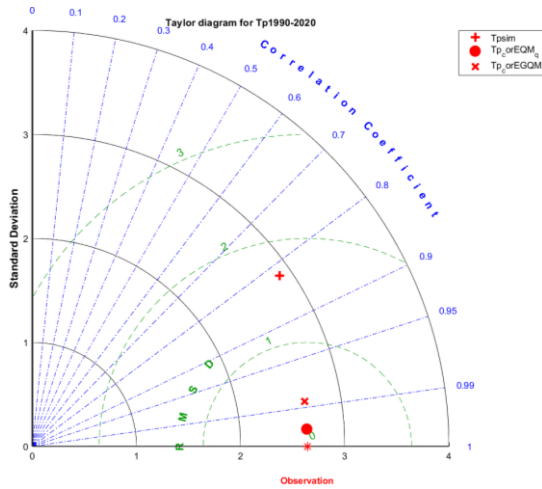


Fig4.12 Taylor diagram for T_p (EGQM)

		Tp(peak period) EGQM			
		Mean [s]	RMSD [s]	PC [-]	σy [s]
Tp	Buoy	9.763	0.000	0.000	2.641
	Simu	10.909	2.019	0.823	2.888
	EQMcor	9.763	0.166	0.998	2.640
	EGQMcor	9.768	0.432	0.987	2.651

Table4.11 statistical value for T_p (EGQM)

The RMSD for peak period using EGQM method is 0.432 that is 2.6 times higher than EQM, and the value of PC in EGQM is 0.987 also not as good as 0.998 in EQM. For mean value and standard deviation, the performance of EQM is a little bit better than that in EGQM, and this can also be seen on Taylor diagram, because the EQM point is closer to observation in contrast with EGQM.

For U_w , its statistical parameters and Taylor diagram are displayed below:

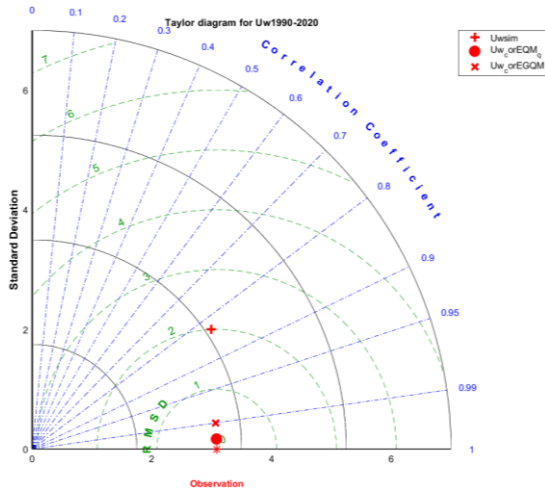


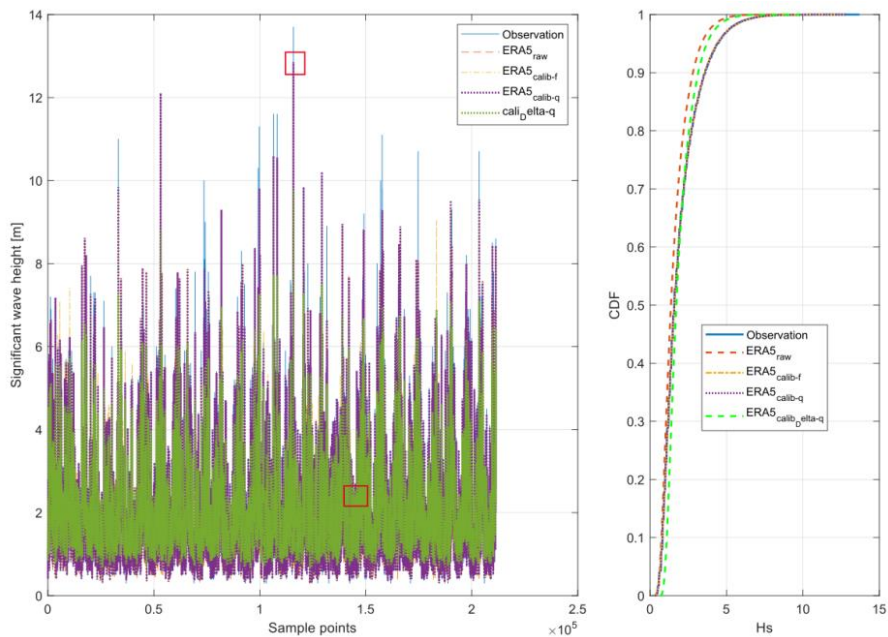
Fig4.13 Taylor diagram for U_w (EGQM)

		Uw(wind speed) EGQM			
		Mean [m/s]	RMSD [m/s]	PC [-]	σ_y [m/s]
Uw	Buoy	5.232	0.000	0.000	3.084
	Simu	6.201	2.222	0.832	3.598
	EQMcor	5.232	0.169	0.998	3.084
	EGQMcor	5.235	0.432	0.990	3.091

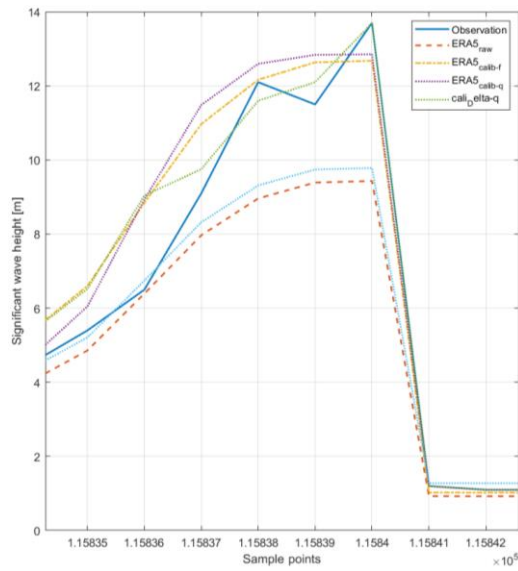
Table4.12 statistical value for U_w (EGQM)

Same situation happened for U_w , higher RMSD are the main difference between EQM and EGQM method just as what we got from H_s and T_p . So a conclusion can be made that in this location, for all three parameters, the EQM (using 99 quantiles) BC method is better than EGQM. As can be seen for the position Bilbao Vizcaya (Gulf of Biscay, north of Spain), three different BC methods have been used and the comparison of these methods is integrated in one plot below:

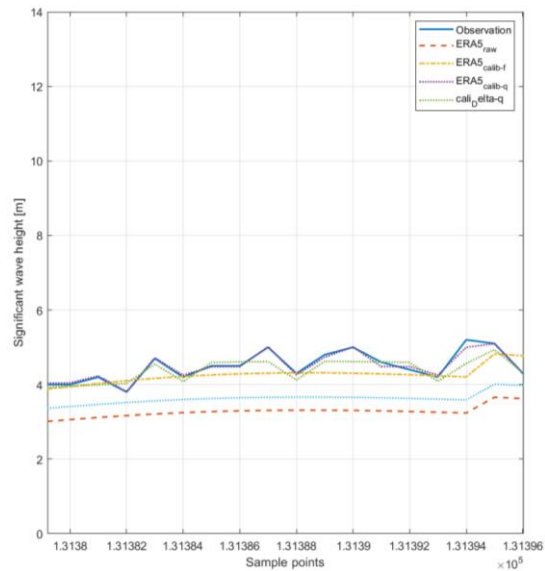
For H_s :



(a) H_s in the whole period (Bilbao Vizcaya)



(b) Hs extreme value (Bilbao Vizcaya)



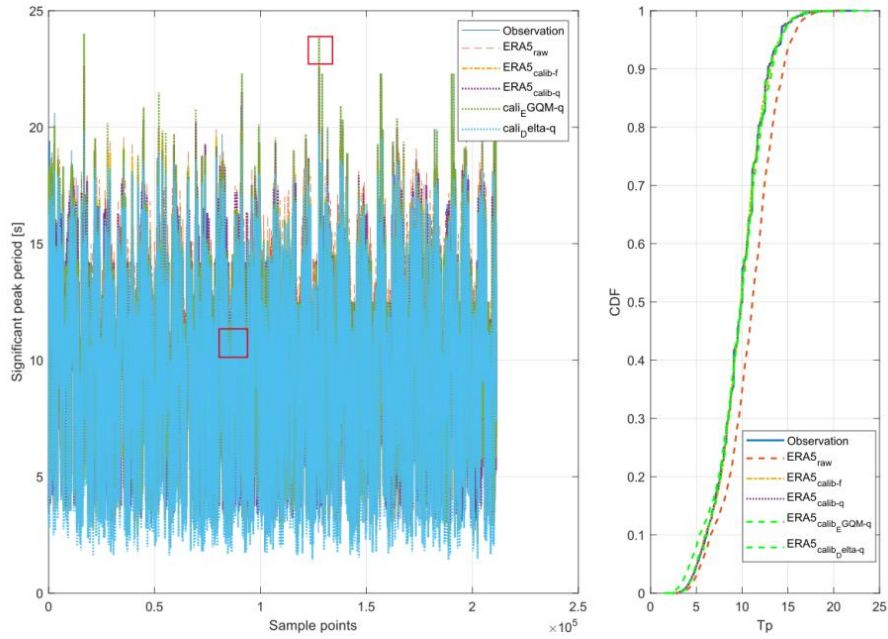
(c) Hs average value (Bilbao Vizcaya)

Fig.4.14 Hs sample for Bilbao Vizcaya

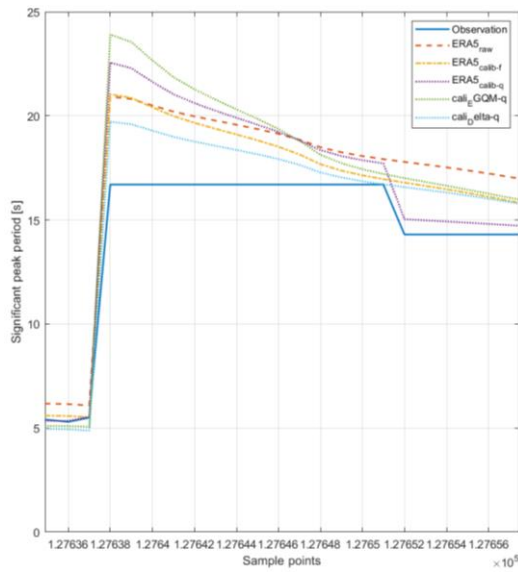
Where Fig.4.14 (a) is the total tendency for three approaches for H_s , Fig.4.14 (b) represent the extreme event of (a) (upper red square of Fig.4.14 (a)), and Fig.4.14 (c) is the part of average condition that selected of (a) (lower red square of Fig.4.14 (a)). As for the extreme values that displayed in Fig.4.14.(b), green dash line, the correction data using EGQM, fits the blue straight (observation) best. The purple line (correction data using EQM) not fit it so good as EGQM, third order is EQM (without using 99 quantiles) and the Delta method is the least similar to the observed data after correction. For instance, if the sample points are 1.0644×10^5 , the observation is 11.1m, EGQM BC value is 11.2m and EQM BC value is 10.55m.

In contrast to extreme value sample, things changes for average sample, in which, the similarity of EQM correction (using 99 quantiles) fits the observation best and EGQM is in the second order, next is EQM correction (without using 99 quantiles) and Delta is the roughest as well. This result is expected, as EGQM improves values higher than 99 quantiles, and most of these data fall in the extreme part, so in extreme areas, EGQM has a good performance. In comparison, EQM correction (using 99 quantiles) is to linearly divide the overall time period into 99 quantiles, and the correction for each part is relatively uniform, so in the average position, EQM has a better performance.

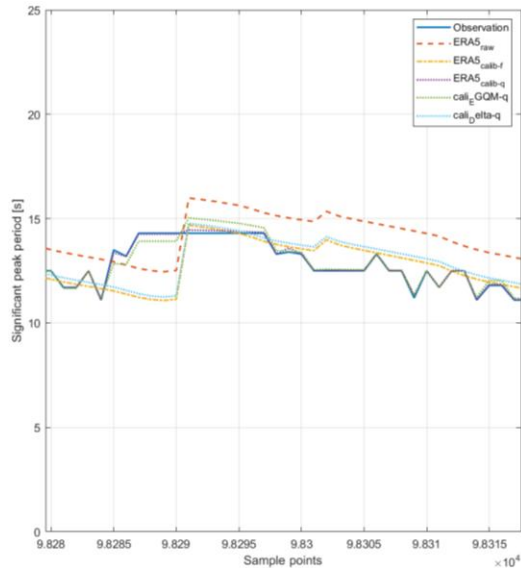
For T_p :



(a) T_p in the whole period (Bilbao Vizcaya)



(b) T_p extreme value (Bilbao Vizcaya)



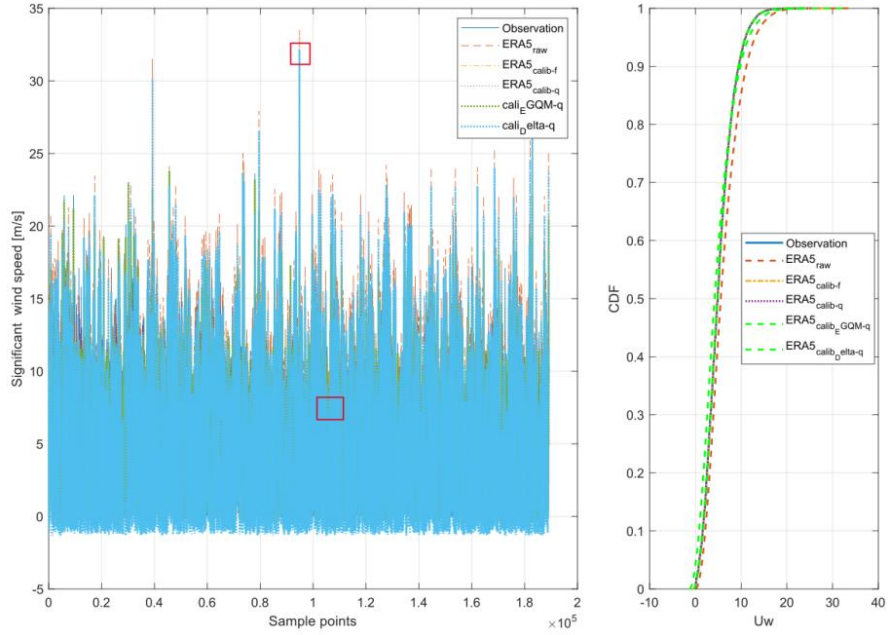
(c) T_p average value (Bilbao Vizcaya)

Fig.4.15 T_p sample for Bilbao Vizcaya

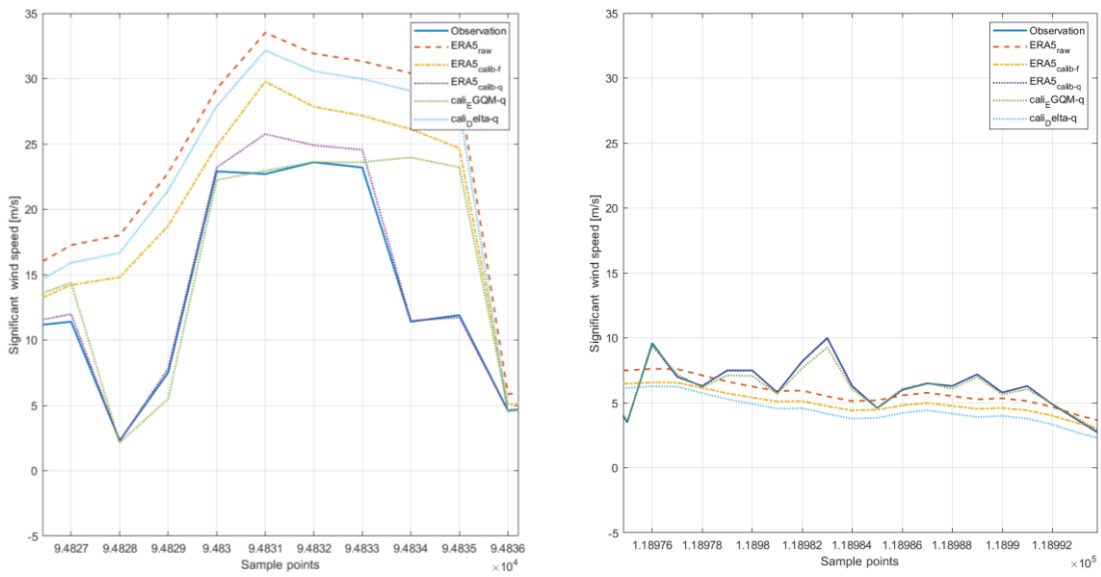
Where (b) represent extreme value of T_p , which is the zoomed in part of upper red square in Fig.4.15 (a), and (c) is the average example of T_p , which is the zoomed in part of lower red square in Fig.4.15 (a). For the extreme sample part of T_p , the order of similarity to observation is

Delta method, EQM (without using 99 quantiles), EQM (using 99 quantiles), and EGQM, this strange situation happened for the highest extreme part, after that, EGQM fit the observation in extreme as well and EQM (using 99 quantiles) is closest to observation in average location.

For U_w :



(a) U_w in the whole period (Bilbao Vizcaya)



(b) U_w extreme value (Bilbao Vizcaya)

(c) U_w average value (Bilbao Vizcaya)

Fig.4.16 U_w sample for Bilbao Vizcaya

Where Fig.4.16 (b) represent extreme value of U_w , which is the zoomed in part of upper red square in Fig.4.16 (a), and Fig.4.16 (c) is the average example of U_w , which is the zoomed in part of lower red square in Fig.4.16 (a). Same situation happened for U_w , there is no special performance as the extreme part of T_p . In this case, EGQM and EQM (using 99quantiles) are the correction samples that fit observation very well, and EGQM is more useful for extreme values, EQM (using 99quantiles) performs better in average part.

From Taylor diagram and sample points figure, the conclusion is that all three bias corrected datasets have better agreement to the observation point compared with the original simulation point, which means BC actually improves the accuracy of the original simulation. For most of the cases, EQM (using 99 quantiles) correction data performs best and the correction of EGQM is more effective when correcting extreme values. While the correction effect of Delta and EQM (without using 99 quantiles) is not so evident, and which one of them is better depends on the quality of the observation data.

4.4 Bias correction in a different location

The study above provides details of three BC methods for analysing three parameters--- H_s , T_p and U_w at Bilbao Vizcaya (north of Spain). Next, same method will be used to analyse Cabo Begur in the east, Cabo Silleiro in the west, and Golf Cadizin in the south, respectively.

4.4.1Cabo Begur (east of Spain)

Same approach has been adopted for observation and simulation data during 2003 to 2020 in Cabo Begur, the datasets after pre-processing is:

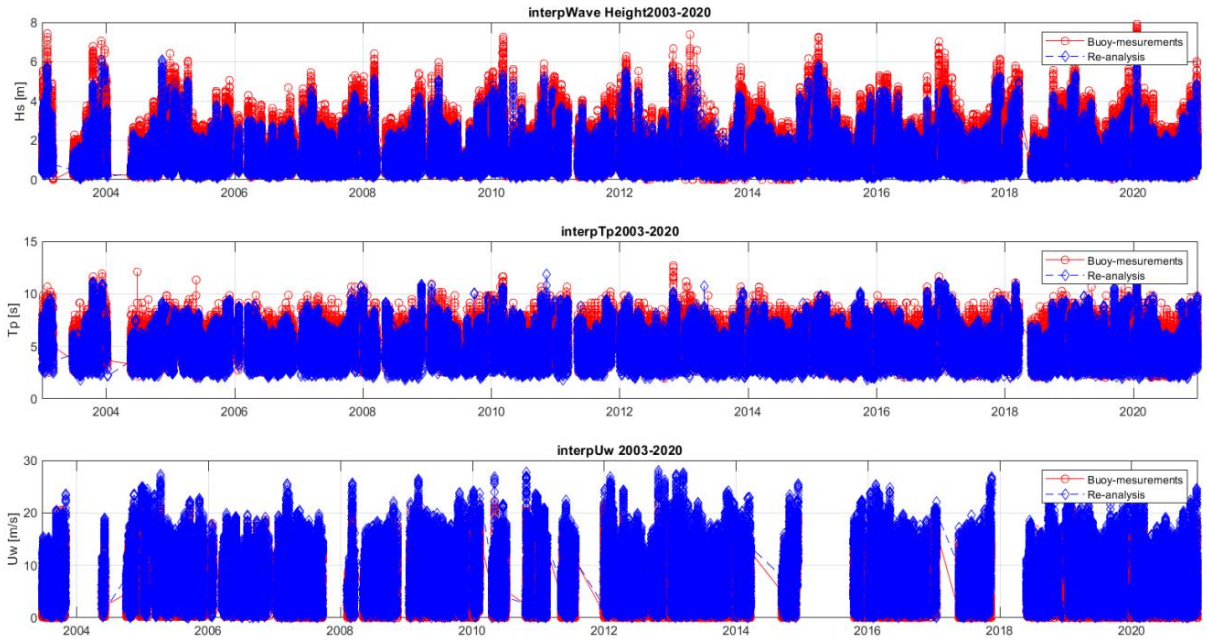


Fig.4.17 datasets after pre-processing for Cabo Begur

4.4.1.1 Wave data

H_s : The 3 BC methods integrated in one single figure:

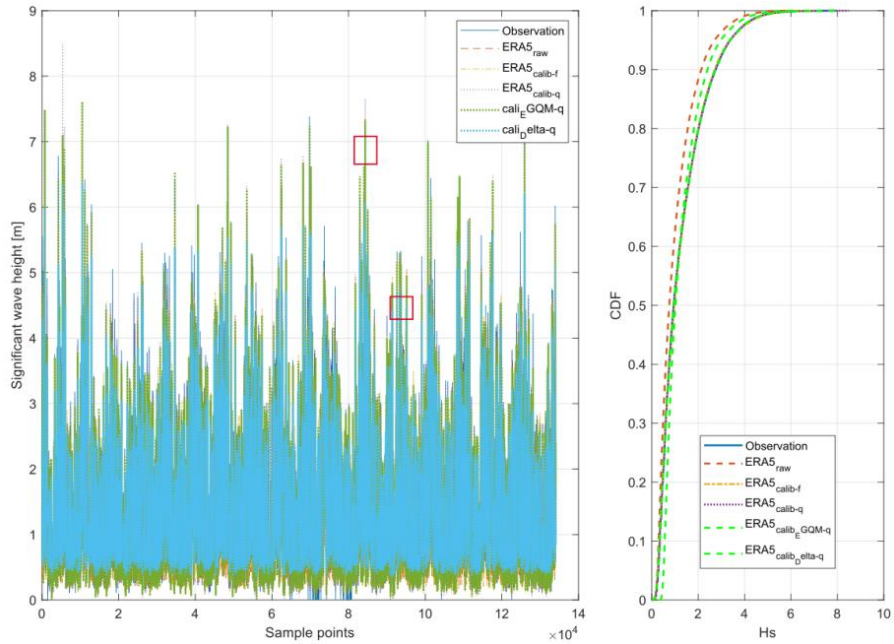


Fig.4.18 H_s in the whole period (Cabo Begur)

The two red squares correspond to the samples of an extreme event and average conditions. The following figures illustrate the different signals for the extreme event (on the left) and the point with average conditions (on the right):

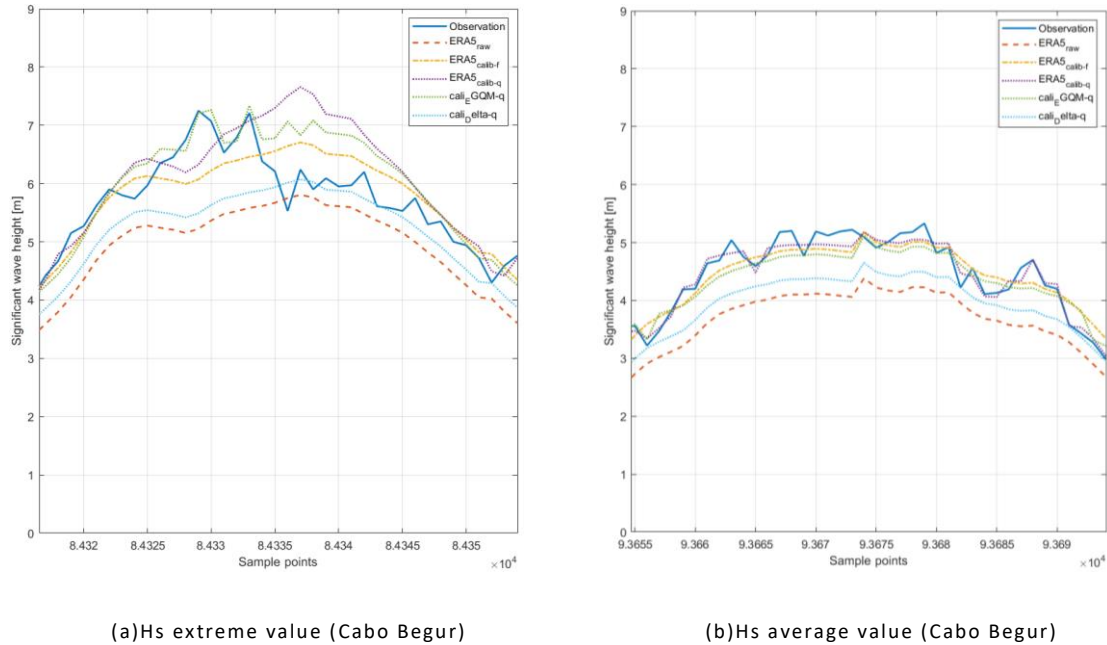


Fig.4.19 H_s extreme and average sample Cabo Begur

Fig.4.19 (a) represent extreme value of H_s , which is the zoomed in part of upper red square in Fig.4.18, and Fig.4.19 (b) is the average example of H_s , which is the zoomed in part of lower red square in Fig.4.8. Same situations are illustrated below where the upper red square is the zoomed out area of extreme part and the lower red square represent the zoomed out area of average part.

The EGQM BC method has significant effect for extreme values correction as can be seen in Fig.4.19 (a) green dash line, and the corrected agreement of EQM (using 99 quantiles) is not so effective. But EQM (using 99 quantiles) performs best for the averaged values as shown in Fig.4.19 (b), while EGQM BC reduce its effectiveness in this regard. Compared with the first two methods, delta and EQM (without using 99 quantiles) are rough, both in extreme and average samples.

Taylor diagram and statistical parameters for H_s using EQM and EGQM in Cabo Begur,

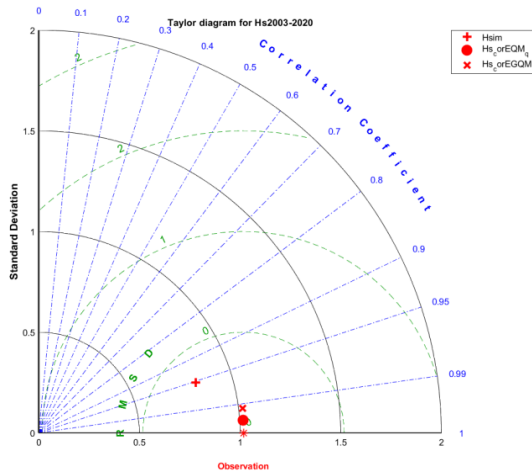


Fig4.20 Taylor diagram for H_s (Cabo Begur)

		Hs(Cabo Begur)			
		Mean [m]	RMSD [m]	PC [-]	σ_y [m]
Hs	Buoy	1.29	0	0	1.02
	Simu	1.02	0.43	0.95	0.82
	EQMcor	1.29	0.06	0.998	1.01
EGQMcor		1.29	0.12	0.992	1.02

Table4.13 statistical value for H_s (Cabo Begur)

From Taylor diagram, the overall performance of EQM (using 99 quantiles) is higher than EGQM, with better RMSD and significantly closing the gap between observation and simulation point.

For T_p : The 3 BC method integrated in one plot:

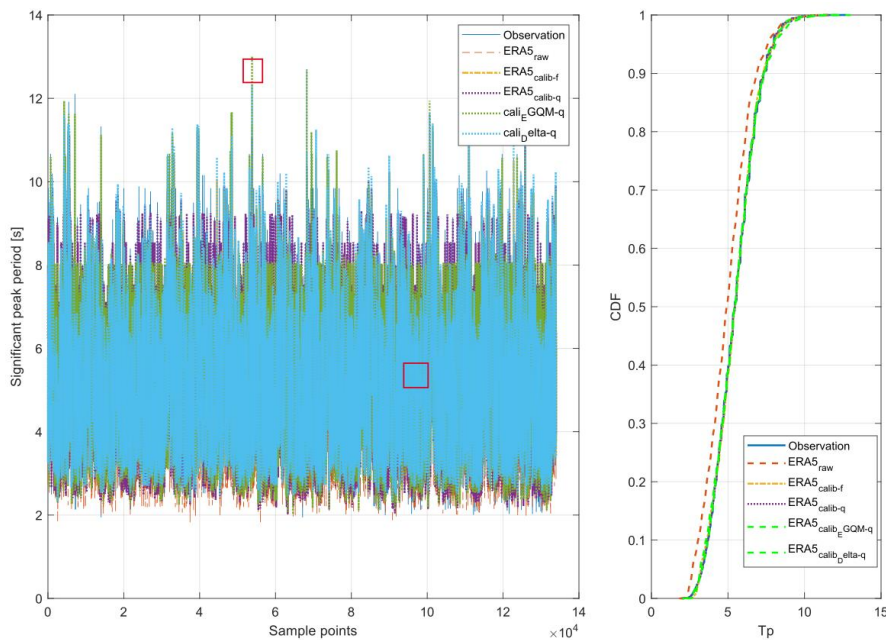


Fig.4.21 T_p in the whole period (Cabo Begur)

Its extreme sample Fig.4.22 (a) and average value sample Fig.4.22(b):

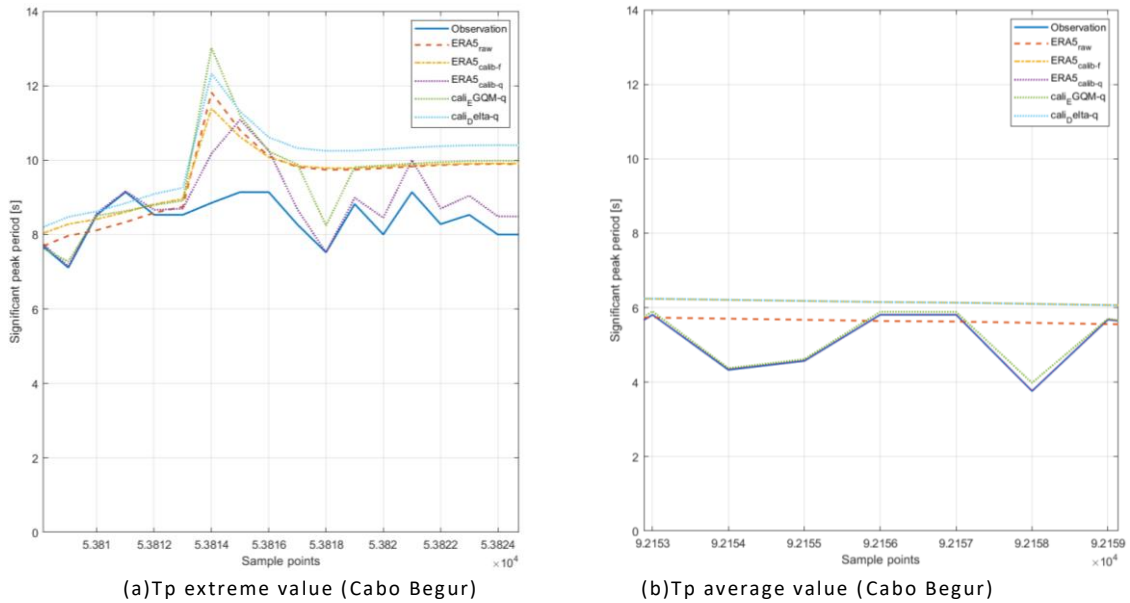


Fig.4.22 T_p extreme and average sample Cabo Begur

Remember the result of T_p in Bilbao Vizcaya, same situation also appear in this location, which can be seen in Fig.4.22 (a), this is because for T_p , the difference between extreme values and average values is not so obvious in the whole dataset, so EGQM is not evident to correct this value part. The trend of average values shows the same thing, where EQM (using 99 quantiles) BC simulation fits observation best, EGQM is the second, next orders are Delta and EQM (without using 99 quantiles). Taylor diagram and statistical parameters for T_p using EQM and EGQM in Cabo Begur,

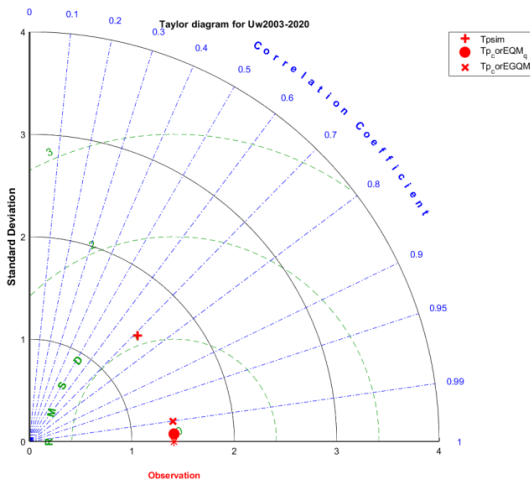


Fig4.23 Taylor diagram for T_p (Cabo Begur)

		T_p (Cabo Begur)			
		Mean [s]	RMSD [s]	PC [-]	σ_y [s]
T_p	Buoy	5.49	0	0	1.41
	Simu	4.98	1.21	0.71	1.48
	EQMcor	5.49	0.07	0.998	1.41
	EGQMcor	5.49	0.19	0.990	1.42

Table4.14 statistical value for T_p (Cabo Begur)

Same condition happened for T_p , compared with others, EQM and EGQM are the first two best choices that have less distance to observation point.

For U_w : The 3 BC methods integrated in a single figure:

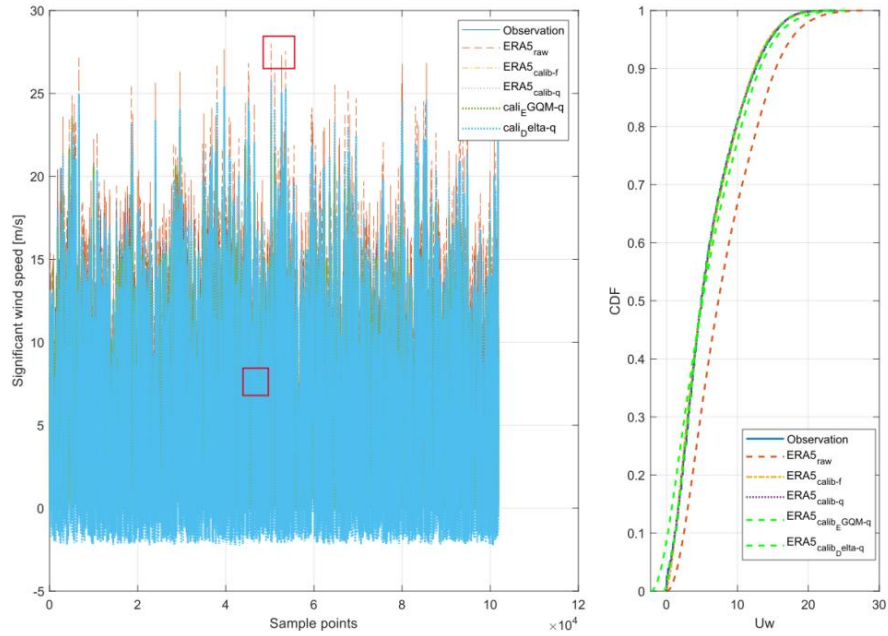
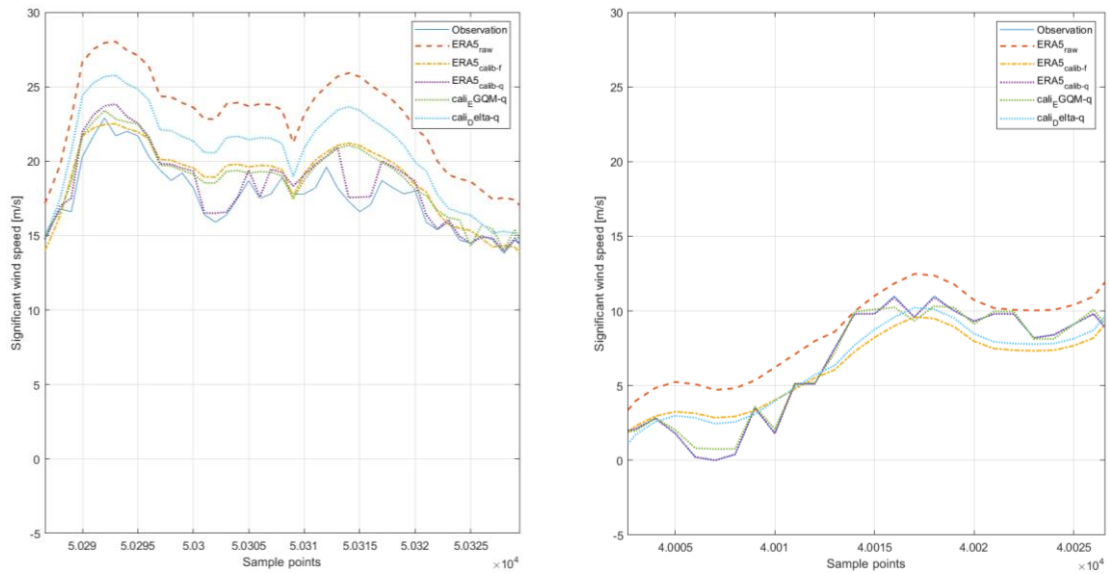


Fig.4.24 U_w in the whole period (Cabo Begur)

Extreme event Fig.4.25 (a) and average condition Fig.4.25 (b) for U_w :



(a) U_w extreme value (Cabo Begur)

(b) U_w average value (Cabo Begur)

Fig.4.25 U_w extreme and average sample Cabo Begur

The value trend of U_w has significant different performance compared with that of T_p , so for extreme sample, EGQM BC simulation performs better and EQM makes good performance for average sample.

Taylor diagram and statistical parameters for U_w using EQM and EGQM in Cabo Begur,

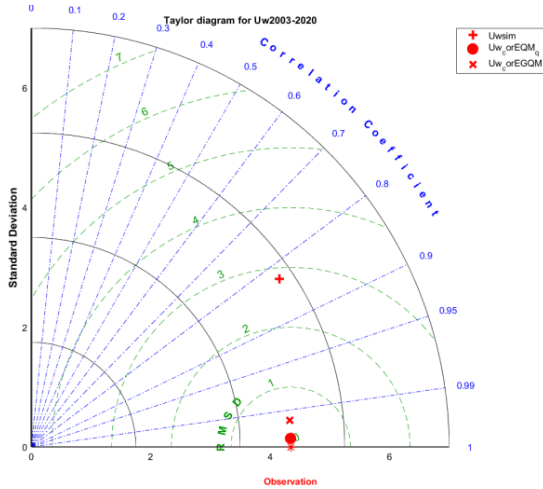


Fig4.26 Taylor diagram for U_w (Cabo Begur)

		Uw(Cabo Begur)			
		Mean [m/s]	RMSD [m/s]	PC [-]	σ_y [m/s]
U_w	Buoy	6.00	0	0	4.34
	Simu	8.26	3.61	0.83	5.02
	EQMcor	6.00	0.14	0.999	4.34
	EGQMcor	6.01	0.44	0.995	4.35

Table4.15 statistical value for U_w (Cabo Begur)

where the red '●' represents the statistical metrics for EQM BC and 'x' for EGQM, where EQM shows a better agreement than EGQM with the observation point.

4.4.2 Cabo Silleiro (west of Spain)

Useful time period that has been chosen for Cabo Silleiro is 2000 to 2020, and the pre-processing dataset:

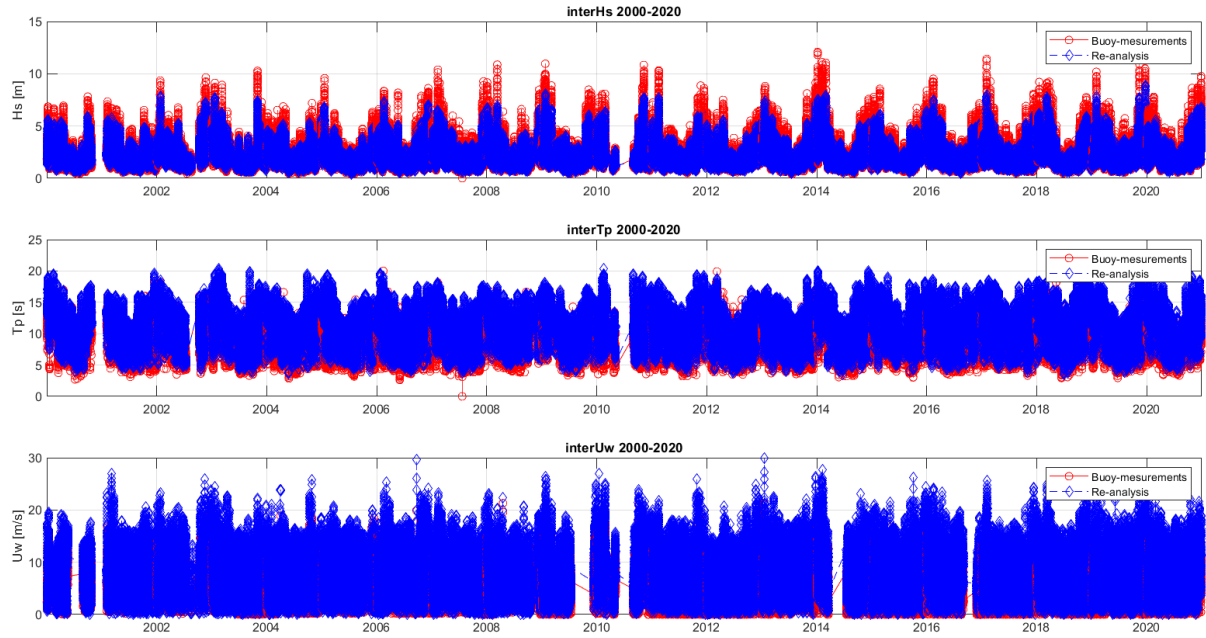


Fig.4.27 datasets after pre-processing for Cabo Silleiro

The total trend of simulation to observation for all three plots are the same, for T_p and U_w , simulation is overestimated compared with observation, while for H_s , simulation is underestimated.

4.4.2.1 Wave data

H_s : The 3 BC methods integrated in a single figure

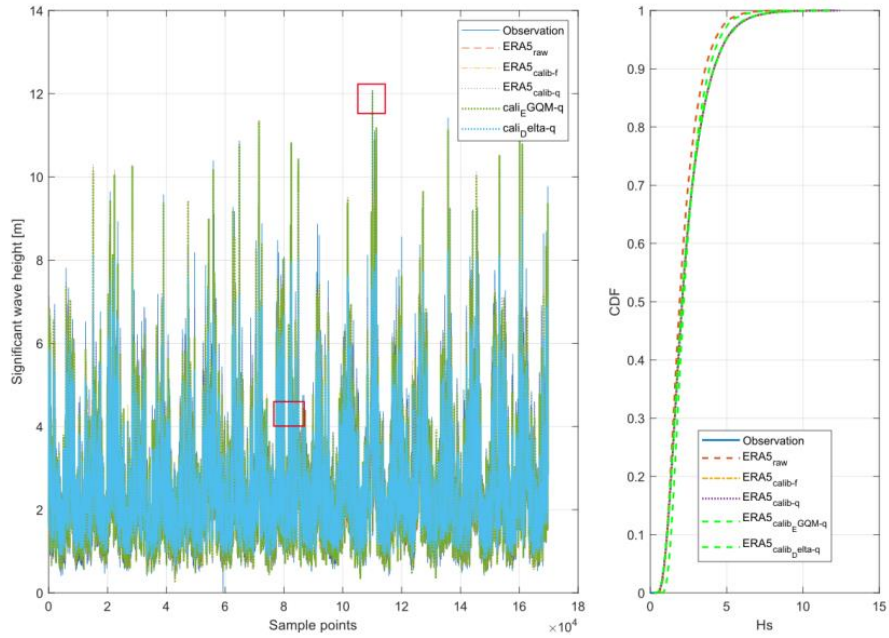
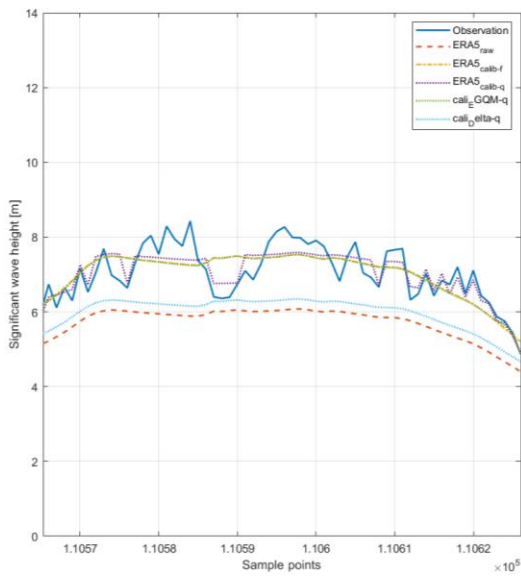
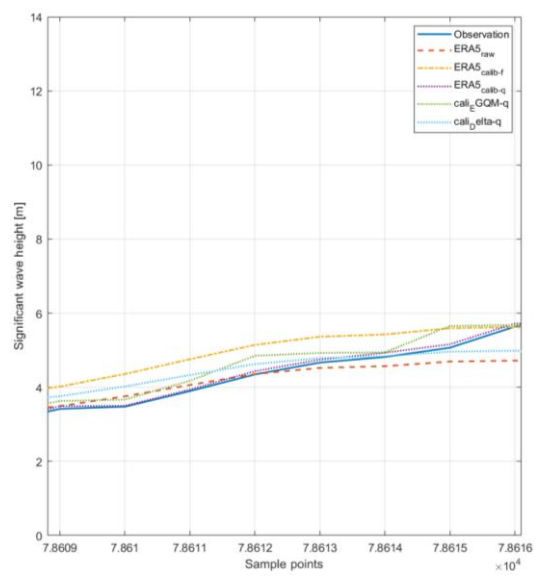


Fig.4.28 Hs in the whole period (Cabo Silleiro)

Where the two red squares correspond to the samples of an extreme event (on the left) and a point of average conditions (on the right).



(a) Hs extreme value (Cabo Silleiro)

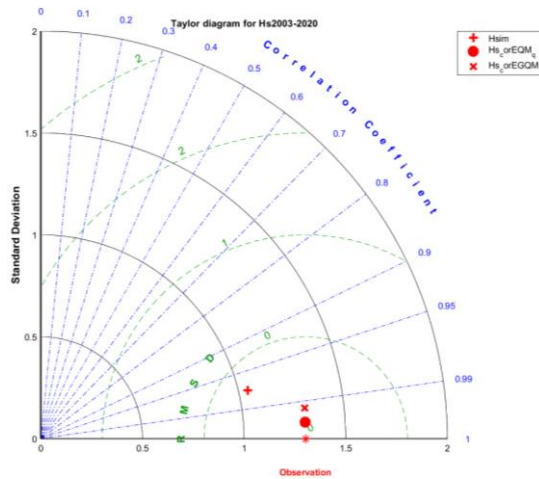


(b) Hs average value (Cabo Silleiro)

Fig.4.29 Hs extreme and average sample Cabo Silleiro

For extreme event Fig.4.29 (a), the domination of EGQM is obvious, no other BC methods perform better than it, and for average condition Fig.4.29(b), EQM (using 99 quantiles) is the best.

Taylor diagram and statistical values:



Hs	Hs (Cabo Silleiro)			
	Mean [m]	RMSD [m]	PC [-]	σy [m]
Buoy	2.40	0	0	1.30
Simu	2.16	0.44	0.97	1.04
EQMcor	2.40	0.08	0.998	1.30
EGQMcor	2.40	0.15	0.993	1.31

Fig.4.30 Taylor diagram for Hs (Cabo Silleiro) Table.4.16 statistical value for Hs (Cabo Silleiro)

Although EGQM BC performs better for extreme values, EQM (using 99 quantiles) still make better correction for the whole time period. Compared EGQM with EQM, with same 'Mean', 'PC' and 'standard deviation', RMSD for EQM (0.08) is lower than that of EGQM that is 0.15.

T_p : The 3 BC methods integrated in a single figure:

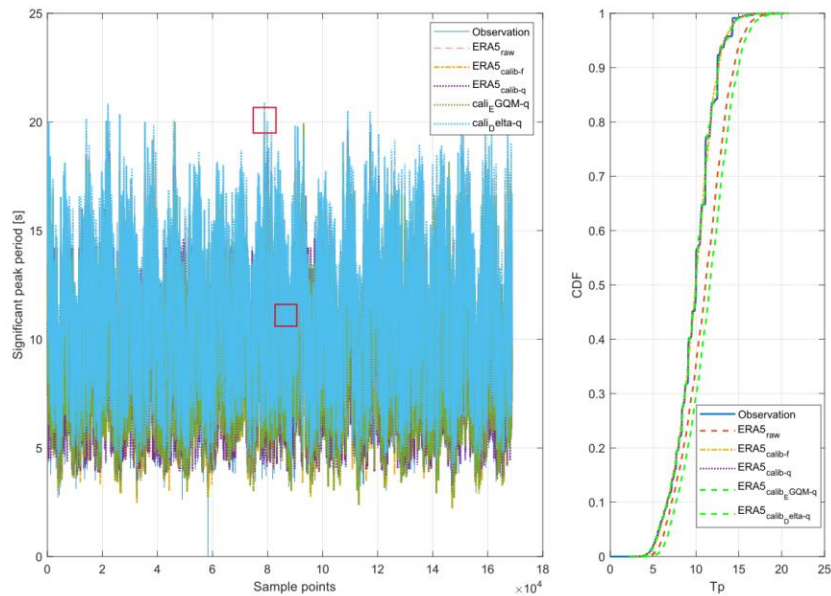


Fig.4.31 T_p in the whole period (Cabo Silleiro)

Extreme event Fig.4.32 (a) and average condition Fig.4.32 (b) for T_p ,

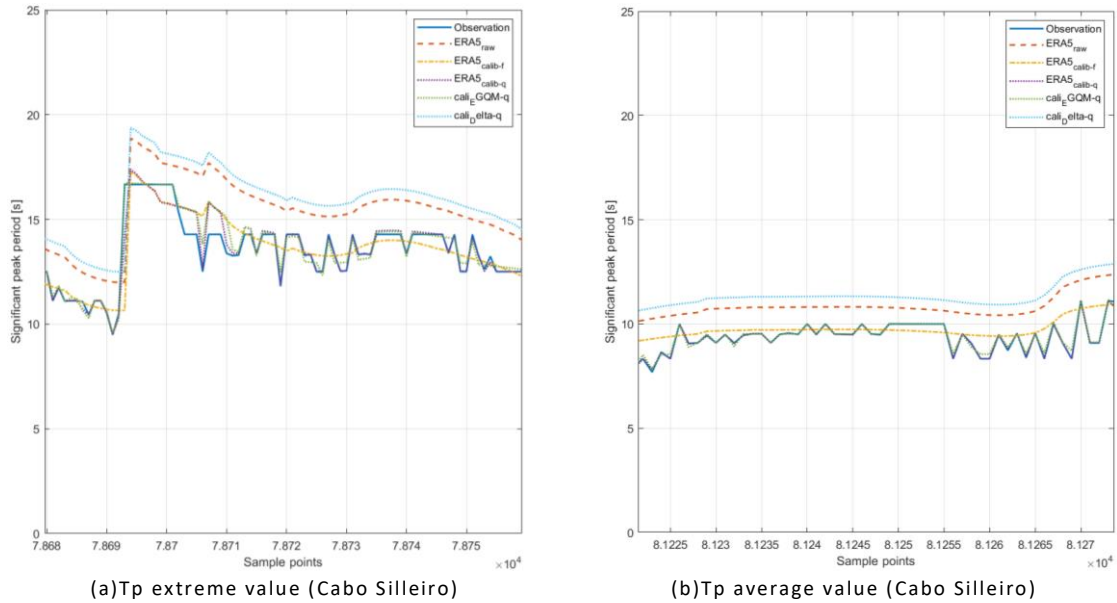


Fig.4.32 T_p extreme and average sample Cabo Silleiro

For extreme values of T_p in Cabo Silleiro, no special point appears, the EGQM fits observation data very well and better than EQM. While EQM shows best correction for average sample, second one is EGQM.

Same situation can also be displayed in Taylor diagram:

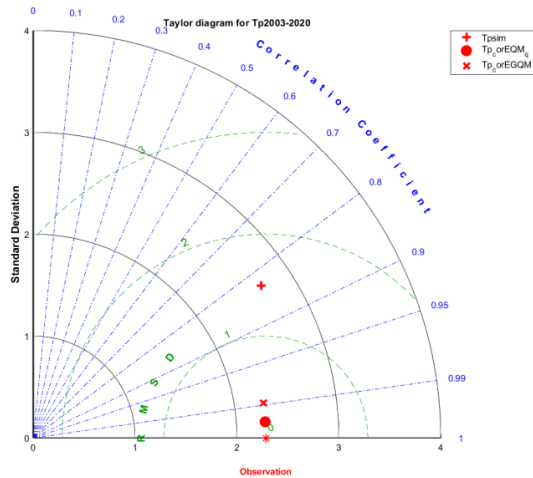


Fig4.33 Taylor diagram for T_p (Cabo Silleiro)

		T_p (Cabo Silleiro)			
		Mean [s]	RMSD [s]	PC [-]	σ_y [s]
T_p	Buoy	9.82	0	0	2.28
	Simu	10.98	1.89	0.83	2.69
	EQMcor	9.82	0.16	0.998	2.28
	EGQMcor	9.82	0.34	0.988	2.28

Table4.17 statistical value for T_p (Cabo Silleiro)

In the whole dataset, EQM always show better correction performance than EGQM, which means it is similar to observation point in Taylor diagram.

4.4.2.2 Wind data

U_w : The 3 BC methods integrated in a single figure:

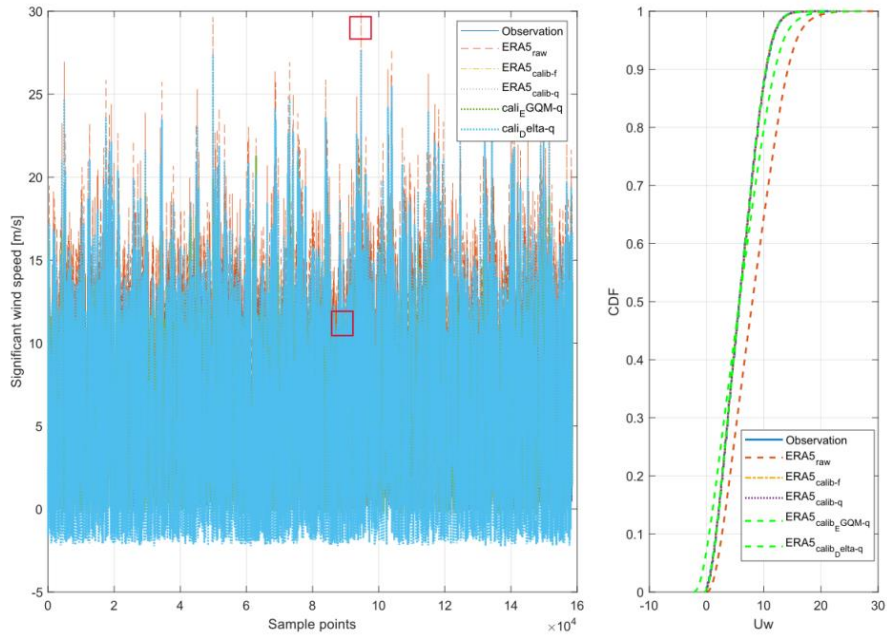


Fig.4.34 U_w in whole time period (Cabo Silleiro)

Details of extreme and average values are showing below:

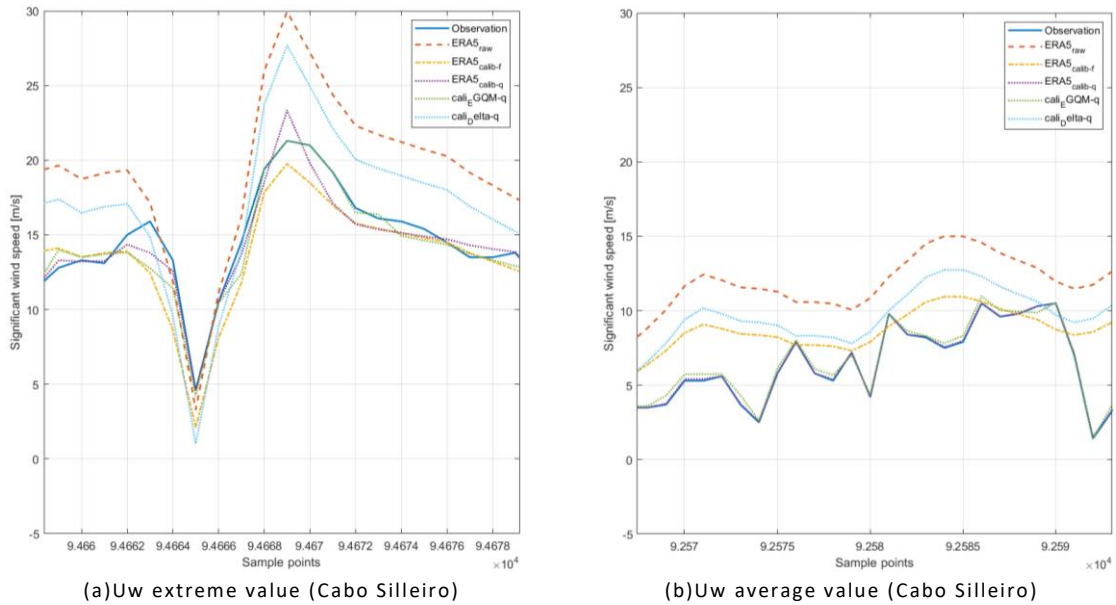
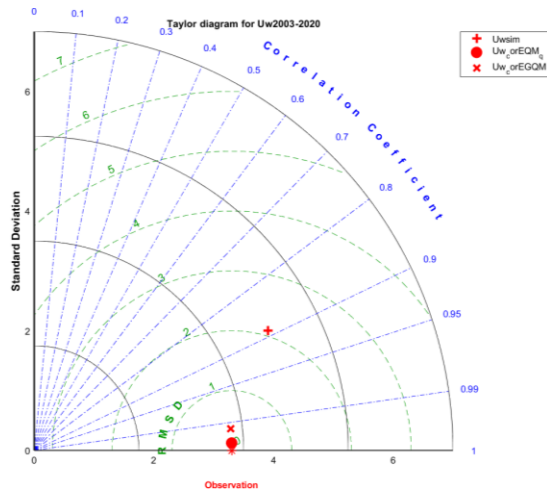


Fig.4.35 U_w extreme and average sample Cabo Silleiro

Displaying from the figure above, purple (EQM) and green dash line (EGQM) are the first two lines that fit blue line (observation) best in both Fig.4.35 (a) and (b). And for sample choosing

from extreme values Fig.4.35 (a), EGQM is most fitable, EQM is more close in average values Fig.4.35(b). Taylor diagram and statistical parameters:



Uw	Uw (Cabo Silleiro)			
	Mean [m/s]	RMSD [m/s]	PC [-]	σ_y [m/s]
Buoy	5.94	0	0	3.30
Simu	8.31	3.17	0.89	4.39
EQMcor	5.94	0.12	0.999	3.30
EGQMcor	5.94	0.37	0.994	3.31

Fig4.36 Taylor diagram for Uw (Cabo Silleiro)

Table4.18 statistical value for Uw (Cabo Silleiro)

The mean value of original simulation is 8.31m/s, after BC, for both using EQM and EGQM, it becomes 5.94m/s that is the same with observation mean. RMSD, PC and standard deviation are all improving significantly compared with original simulation. As for the whole dataset, EQM also performs better than EGQM, like what is showing before.

4.4.3 Gulf Cadiz (south of Spain)

For Gulf Cadiz, meaningful time period has also been chosen during 2000 to 2020, pre-processing observation and simulation are:

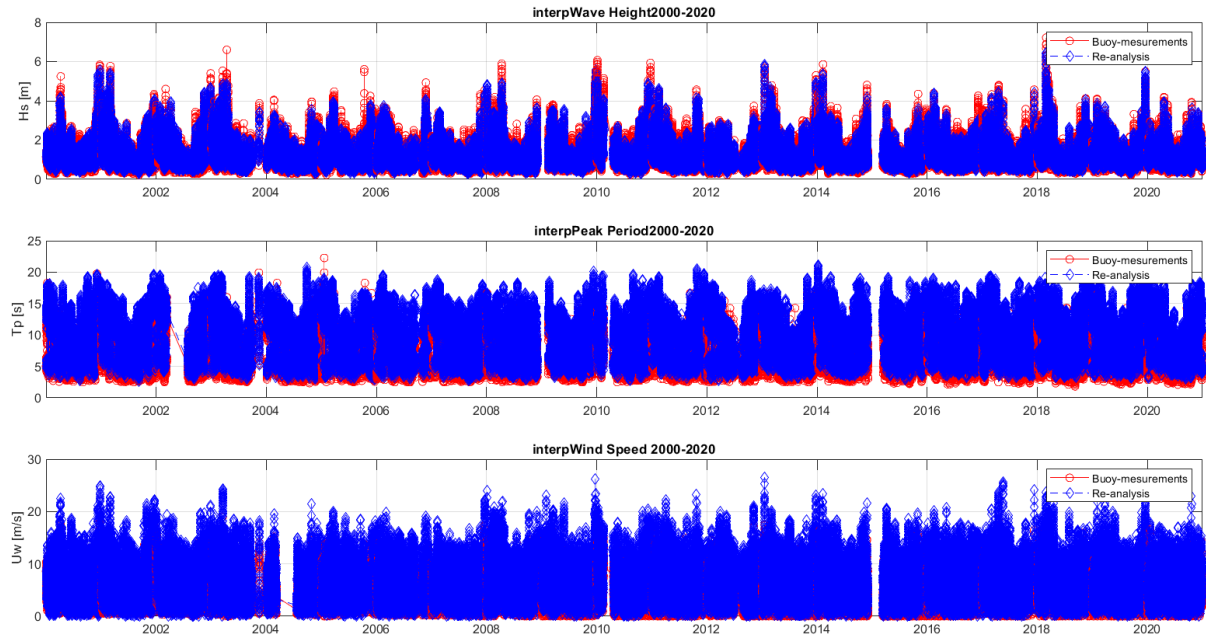


Fig.4.37 datasets after pre-processing for Gulf Cadiz

Where for T_p and U_w , original simulation overestimate the observation value, and in H_s figure, original simulation underestimate the observation.

4.4.3.1 Wave data

H_s : The 3 BC methods integrated in a single figure:

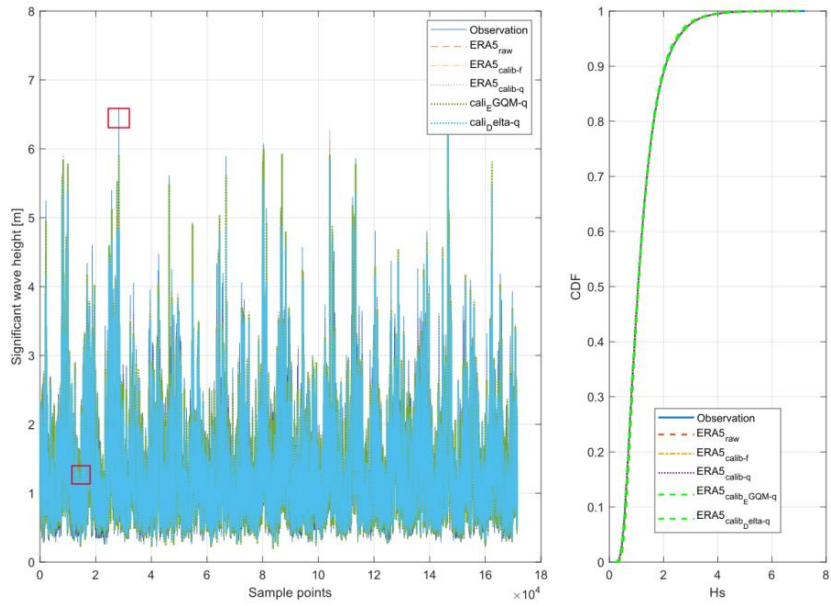
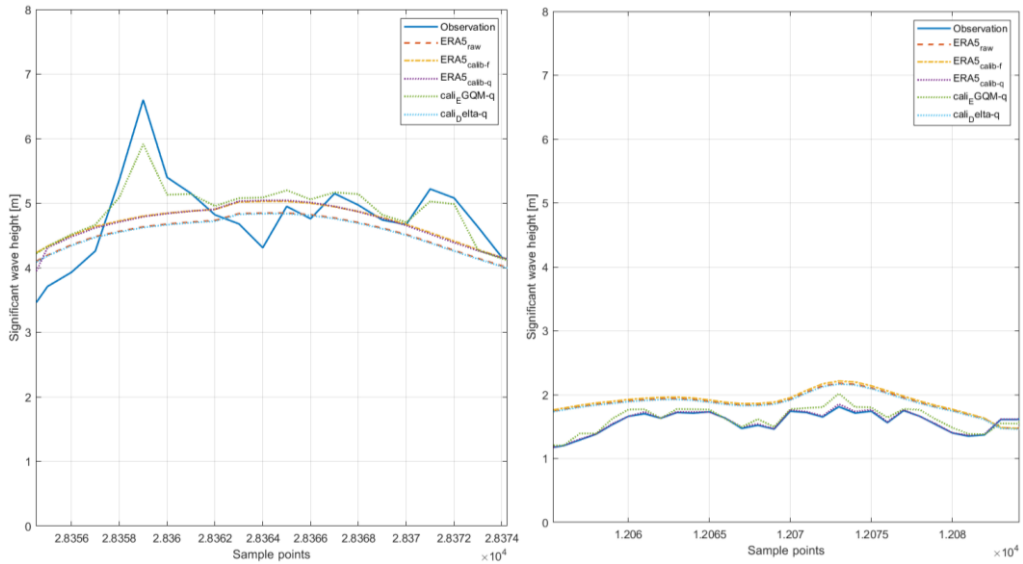


Fig.4.38 H_s in whole time period (Gulf Cadiz)

Extreme event Fig.4.39 (a) and average sample Fig.4.39 (b) are showing below:



(a) H_s extreme value (Gulf Cadiz)

(b) H_s average value (Gulf Cadiz)

Fig.4.39 H_s extreme and average sample Gulf Cadiz

The result of corrected H_s in Gulf Cadiz has no special changes, in which EGQM fit observation for extreme values and EQM performs best for average values.

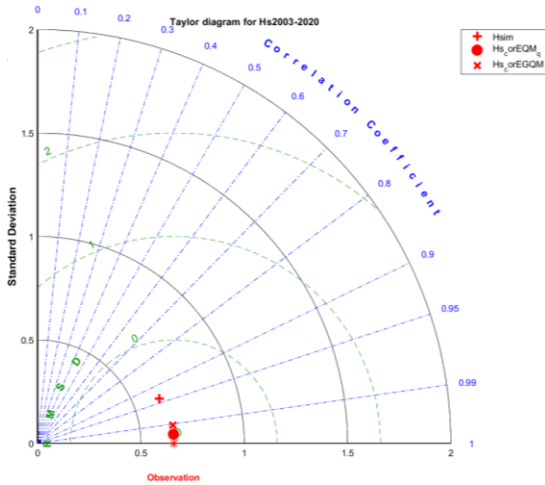


Fig4.40 Taylor diagram for Hs (Gulf Cadiz)

		Hs (Cabo Silleiro)			
		Mean [m]	RMSD [m]	PC [-]	σ_y [m]
Hs	Buoy	1.22	0	0	0.66
	Simu	1.23	0.23	0.94	0.63
	EQMcor	1.22	0.04	0.998	0.66
	EGQMcor	1.22	0.09	0.991	0.66

Table4.19 statistical value for Hs (Gulf Cadiz)

Same situation is showing in Taylor diagram where red '●' represents the statistical metrics for EQM BC and 'x' for EGQM.

T_p : The 3 BC methods integrated in a single figure:

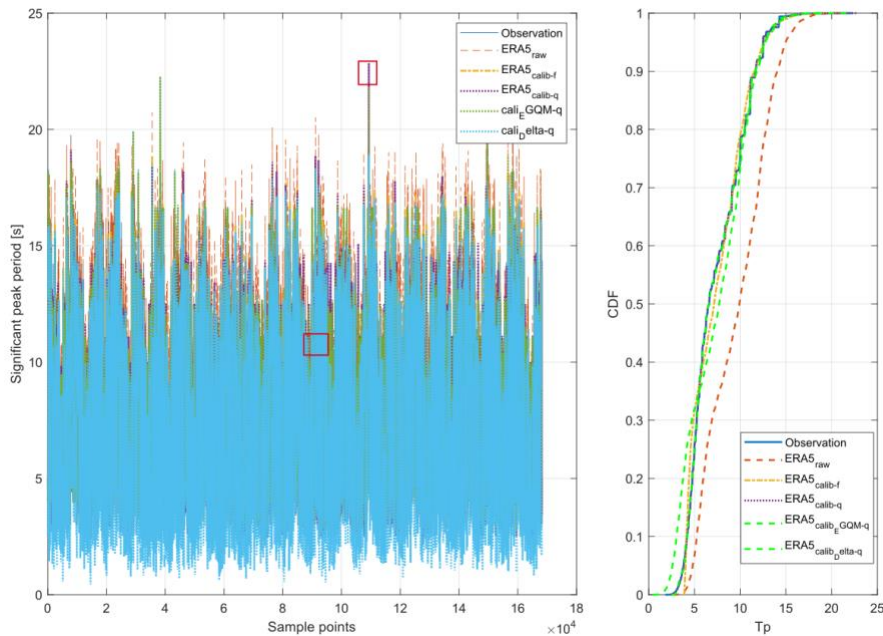
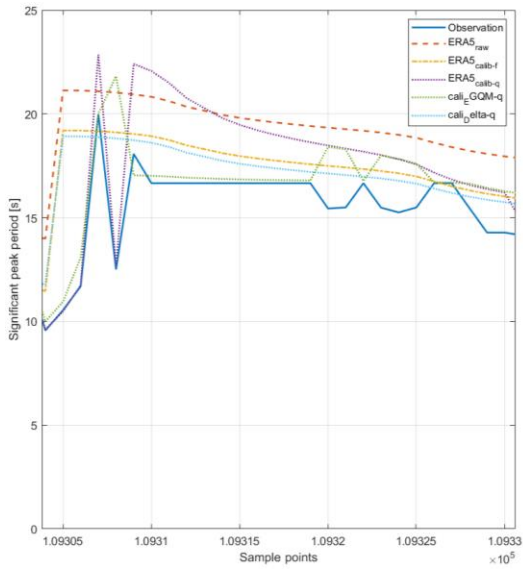
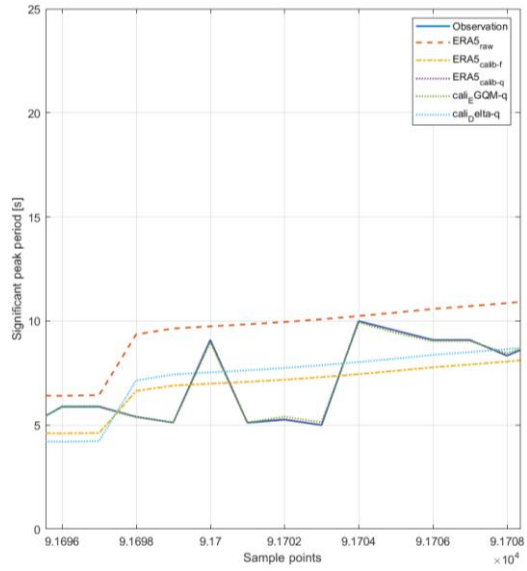


Fig.4.41 T_p in whole time period (Gulf Cadiz)

Fig.4.41 is the figure for whole dataset, extreme sample Fig.4.42 (a) and average sample Fig.4.42 (b) are showing below:



(a) Tp extreme value (Gulf Cadiz)



(b) Tp average value (Gulf Cadiz)

Fig.4.42 Tp extreme and average sample Gulf Cadiz

Taylor diagram and statistical parameters:

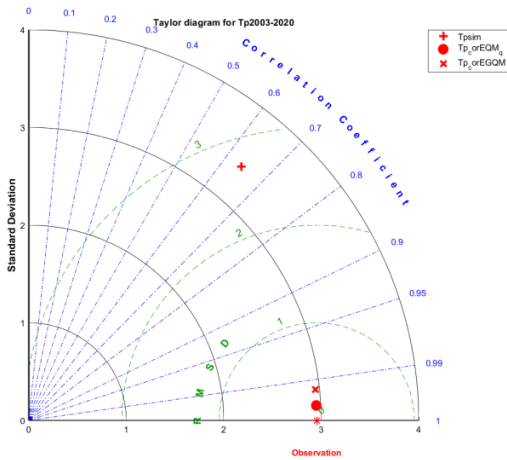


Fig4.43 Taylor diagram for Tp (Gulf Cadiz)

Tp	Tp (Cabo Silleiro)				
	Mean [m]	RMSD [m]	PC [-]	oy [m]	
Buoy	7.47	0	0	2.95	
Simu	9.68	3.50	0.64	3.40	
EQMcor	7.47	0.15	0.998	2.95	
EGQMcor	7.47	0.32	0.994	2.95	

Table4.20 statistical value for Tp (Gulf Cadiz)

Same situation happened like what we got before that is in whole data, EQM BC performs better than EGQM and EGQM performs better than any other BC methods.

4.4.3.2 Wind data

U_w : The 3 BC methods integrated in a single figure:

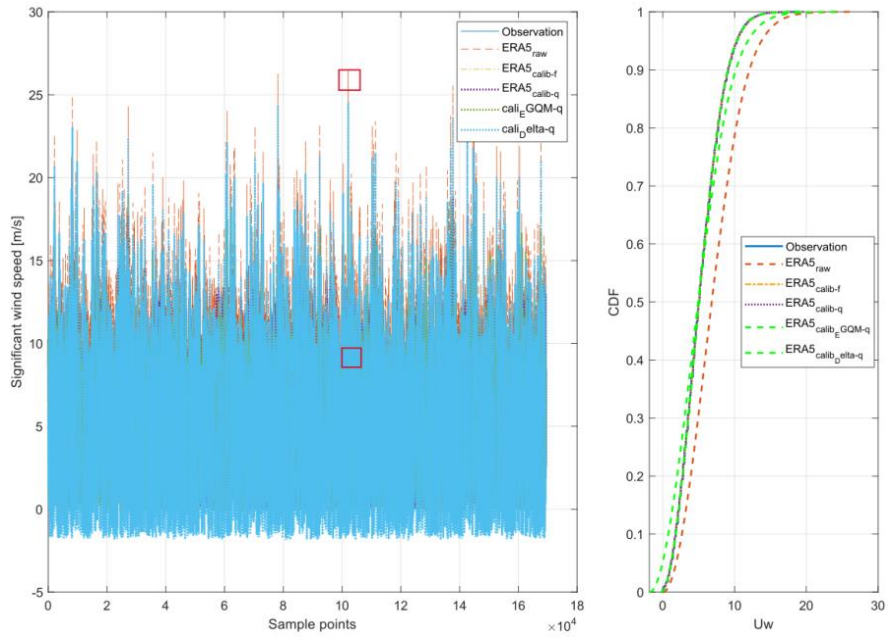
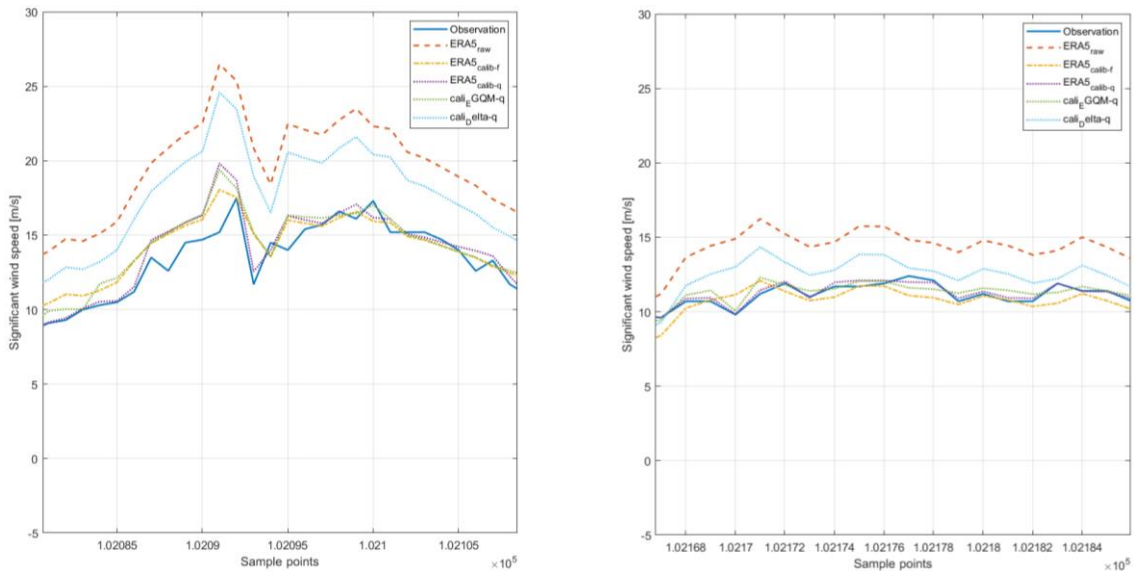


Fig.4.44 U_w in whole time period (Gulf Cadiz)

As we did before, extreme event Fig.4.45 (a) and average condition Fig.4.45 (b) has been illustrated below:



(a) U_w extreme value (Gulf Cadiz)

(b) U_w average value (Gulf Cadiz)

Fig.4.45 U_w extreme and average sample Gulf Cadiz

Where for extreme event Fig.4.45 (a), EGQM showing the best overlap with observation, EQM is the second one. For average condition Fig.4.45 (b), EQM performs best correction agreement and EGQM is the second. Taylor diagram and statistical parameters:

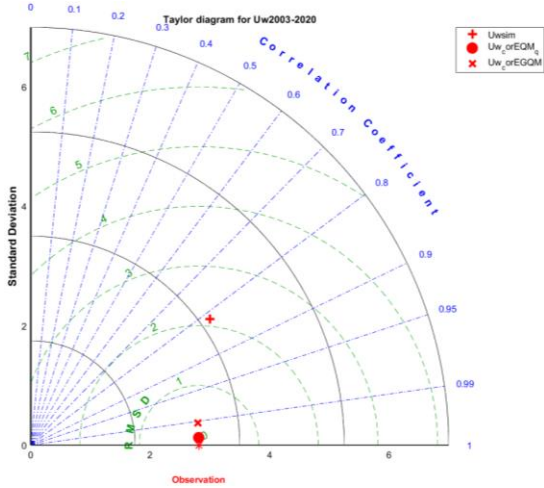


Fig4.46 Taylor diagram for Uw (Gulf Cadiz)

Uw	Uw (Cabo Silleiro)				
		Mean [m]	RMSD [m]	PC [-]	σ_y [m]
Buoy		5.29	0	0	2.82
Simu		7.18	2.84	0.82	3.67
EQMcor		5.29	0.13	0.999	2.82
EGQMcor		5.29	0.38	0.992	2.82

Table4.21 statistical value for Uw (Gulf Cadiz)

4.5 Summary of results for four locations

For a more intuitive comparison of the 4 BC methods in four different locations, all their data are summarized in Table4.22, where ‘bias’ is the difference between observation mean and simulation mean, ‘RMSD’ refers to root mean square deviation, ‘PC’ is the correction coefficient and ‘SD’ represents standard deviation. From the Table4.22, the shadow parts illustrate the best value of the corresponding parameter, and for 48 different variables, 45 values are obtained from EQM (using 99 quantiles), and the other 3 different data are also very close compared to the corresponding EQM data, which means in this thesis, the chosen locations around Spain, EQM (using 99 quantiles) is the best Bias Correction method that can be used.

		Gulf Biscay				Cabo Begur				Cabo Silleiro				Gulf Cadiz			
		Bias	RMSD	PC	SD	Bias	RMSD	PC	SD	Bias	RMSD	PC	SD	Bias	RMSD	PC	SD
Hs	Obs	-	0	0	1.22	-	0	0	1.02	-	0	0	1.30	-	0	0	0.66
	Ori sim	0.34	0.547	0.966	0.88	0.27	0.43	0.950	0.82	0.24	0.44	0.97	1.04	-0.01	0.23	0.94	0.63
	Delta	0.01	0.45	0.965	0.89	0	0.34	0.954	0.82	-0.03	0.37	0.974	1.04	0	0.23	0.939	0.63
	EQM	0	0.32	0.997	1.22	0	0.31	0.954	1.02	0	0.30	0.974	1.30	0	0.23	0.939	0.66
	EQM_99	0	0.08	0.997	1.22	0	0.06	0.998	1.01	0	0.08	0.998	1.30	0	0.04	0.998	0.66
	EGQM	0	0.15	0.992	1.22	0	0.12	0.992	1.02	0	0.15	0.993	1.31	0	0.09	0.991	0.66
Tp	Obs	-	0	0	2.64	-	0	0	1.41	-	0	0	2.28	-	0	0	2.95
	Ori sim	-1.15	2.02	0.82	2.89	0.51	1.21	0.71	1.48	-1.16	1.89	0.83	2.69	-2.21	3.50	0.64	3.40
	Delta	0.06	1.69	0.819	2.91	0	1.10	0.709	1.48	-1.67	2.25	0.828	2.69	0	2.71	0.642	3.40
	EQM	0	1.57	0.999	2.64	0	1.08	0.709	1.41	0	1.34	0.828	2.28	0	2.49	0.642	2.93
	EQM_99	0	0.17	0.998	2.64	0	0.07	0.998	1.41	0	0.16	0.998	2.28	0	0.15	0.998	2.95
	EGQM	-0.01	0.43	0.987	2.65	0	0.19	0.990	1.42	0	0.34	0.988	2.28	0	0.32	0.994	2.95
Uw	Obs	-	0	0	3.08	-	0	0	4.34	-	0	0	3.30	-	0	0	2.82
	Ori sim	-0.97	2.22	0.83	3.60	-2.26	3.61	0.83	5.02	-2.37	3.17	0.89	4.39	-1.89	2.84	0.82	3.67
	Delta	0.04	1.94	0.843	3.59	0	2.82	0.834	5.02	-0.12	2.09	0.890	4.39	0	2.12	0.818	3.67
	EQM	0	1.80	0.998	3.08	0	2.50	0.834	4.34	0	1.55	0.890	3.30	0	1.70	0.818	2.82
	EQM_99	0	0.17	0.999	3.08	0	0.14	0.999	4.34	0	0.12	0.999	3.30	0	0.13	0.999	2.82
	EGQM	-0.01	0.43	0.990	3.09	-0.01	0.44	0.995	4.35	0	0.37	0.994	3.31	0	0.38	0.992	2.82

Table4.22 Summary of results for four locations

It shows that by using EQM (using 99 quantiles), the mean differences between corrected simulation and observation are all 0, and correction coefficients are all higher than 0.99, which have good agreement with observation data.

5. Conclusion and future work

This work has discussed the performance of simulation climate data after three kinds of bias correction techniques (Delta, The Empirical Quantile Mapping method (EQM) and the Empirical Gumbel Quantile Mapping method (EGQM)) in four different locations around Spain, in order to find a reasonable correction method to predict and calculate the local ocean energy resource. The results obtained allowing us comparing the performance of three bias correction approaches and find a better way to perform the correction for datasets of significantly different resource characteristics. Hence, the main conclusions are:

1. After going through three different bias correction (BC) methods, each method improves the quality of the original simulation data, approaching to the observation data, which means all approaches are meaningful and useful.
2. The two most effective correction methods to the original simulation data are EQM (using 99 quantiles) and EGQM, while the Delta method and EQM (without using 99 quantiles) perform rougher than the above two.
3. Learning from data plots in one figure, EGQM performs very well for extreme values, while EQM fits best the observation data for average values. This is because EGQM uses a Standard Gumbel distribution that focuses on the highest (+99th) quantiles and EQM uses evenly distributed 99 quantiles.
4. From Taylor diagram, in the whole dataset, the most effective method is EQM (using 99 quantiles), its parameter point is closet to observation, and EGQM is in the second rank.

According to our conclusion, for different locations and situations, if extreme weather occurs frequently in a place, EGQM should be the best choice to correct simulation data. And if the highest peak period in a certain place does not change so much compared with the average, then even if extreme sample is selected, EQM (using 99 quantiles) can still play a better correction effect, like the extreme sample of T_p in Cabo Begur.

This thesis provides an idea of what kind of bias correction methods can be used for climate analysis and prediction. The next work should be using this idea to predict climate condition and compute ocean energy in certain area, and finally build a renewable energy farm for electricity production.

Acknowledge

On the completion of the thesis, I want to say thank you to my thesis supervisors, MARKEL PENALBA RETES and GIORGI GIUSEPPE, for their careful guidance of my graduation thesis in the past few months.

Special thanks to my parents and everyone who believed in me and inspired me to do even better, thanks to my colleagues for their company with me abroad.

Thanks to all professors who have ever taught me during my graduate study, I would like to thank those who helped me with my graduate study and thesis during this period.

Reference

1. Lemos, G., Semedo, A., Dobrynin, M., Behrens, A., Staneva, J., Bidlot, J.-R., Miranda, P., 2019. Mid-twenty-first century global wave climate projections: results from a dynamic CMIP5 based ensemble. *Glob. Planet. Chang.* 172, 69–87.
2. Gil Lemos, Melisa Menendez, Alvaro Semedo, Paula Camus, Mark Hemer, Mikhail Dobrynin, Pedro M.A. Miranda. On the need of bias correction methods for wave climate projections. *Global and Planetary Change* 186.
3. M. Turco, M. C. Llasat, S. Herrera , and J. M. Gutiérrez, 2016. Bias correction and downscaling of future RCM precipitation projections using a MOS-Analog technique. *Journal of Geophysical Research: Atmospheres* 10.1002/2016JD025724
4. Douglas Maraun. Bias Correcting Climate Change Simulations - a Critical Review. DOI 10.1007/s40641-016-0050-x
5. Ramirez-Villegas J and Challinor A 2012 Assessing relevant climate data for agricultural applications *Agricult. For. Meteorol.* 161 26-45
6. Hay, L.E., Wilby, R.J.L., Leavesley, G.H., 2000. A comparison of delta change and downscaled GCM scenarios for three mountainous basins in the United States. *J. Am. Water Resour. Assoc.* 36, 387–397.
7. Piani, C., Weedon, G.P., Best, M., Gomes, S.M., Viterbo, P., Hagemann, S., Haerter, J.O., 2010. Statistical bias correction of global simulated daily precipitation and temperature for the application of hydrological models. *J. Hydrol.* 395, 199-215.
8. Hay, L.E., Clark, M.P., 2003. Use of statistically and dynamically downscaled atmospheric model output for hydrologic simulations in three mountainous basins in the western United States. *J. Hydrol.* 282, 56 – 75.
9. von Storch, H., Zwiers, F.W., 1999. *Statistical Analysis in Climate Research*. Cambridge University Press, pp. 484.

10. Minguéz, R., Espejo, A., Tomás, A., Méndez, F.J., Losada, I.J., 2011. Directional calibration of wave reanalysis databases using instrumental data. *J. Atmos. Ocean. Technol.* 28, 1466–1485.
11. Déqué, M., 2007. Frequency of precipitation and temperature extremes over France in an anthropogenic scenario: model results and statistical correction according to observed values. *Glob. Planet. Chang.* 57, 16–26.
12. Boé, J., Terray, L., Habets, F., Martin, C., 2007. Statistical and dynamical downscaling of the Seine basin climate for hydro-meteorological studies. *Int. J. Climatol.* 27 (12), 1643–1655.
13. Amengual, A., Homar, V., Romero, R., Alonso, S., Ramis, C., 2012. A statistical adjustment of regional climate model outputs to local scales: application to platja de palma, Spain. *J. Clim.* 25, 939–957.
14. Sharma, D., Das Gupta, A., Babel, M.S., 2007. Spatial disaggregation of bias-corrected GCM precipitation for improved hydrologic simulation: Ping river basin, Thailand. *Hydrol. Earth Syst. Sci.* 11, 1373–1390.
15. Teutschbein, C., Seibert, J., 2012. Bias correction of regional climate model simulations for hydrological climate-change impact studies: review and evaluation of different methods. *J. Hydrol.* 456–457.
16. Panofsky, H.A., Brier, G.W., 1968. Some applications of statistics to meteorology. In: *Earth and Mineral Sciences Continuing Education*. College of Earth and Mineral Sciences.
17. Hemer, M.A., McInnes, K., Ranasinghe, R., 2012. Climate and variability bias adjustment of climate model-derived winds for a southeast Australian dynamical wave model. *Ocean Dyn.* 62 (1), 87–104.
18. Applequist, S., 2012. Wind rose bias correction. *J. Appl. Meteorol. Climatol.* 51, 1305–1309.
19. Terink, W., Hurkmans, R.T.W.L., Torfs, P.J.J.F., Uijlenhoet, R., 2009. Bias correction of temperature and precipitation data for regional climate model application to the Rhine basin. *Hydrol. Earth Syst. Sci. Discuss.* 6, 5377–5413.

20. Charles, E., Idier, D., Delecluse, P., Déqué, M., Le Cozannet, G., 2012. Climate change impact on waves in the Bay of Biscay, France. *Ocean Dyn.* 62 (6), 831–848.
21. Douglas Maraun, 2016. Bias Correcting Climate Change Simulations - a Critical Review. *Current Climate Change Reports* volume 2, 2016, 211–220.
22. ERA5 hourly data on pressure levels from 1959 to present.
23. Teutschbein, C.; Seibert, J. Regional climate models for hydrological impact studies at the catchment scale: A review of recent modeling strategies. *Geogr. Compass* 2010, 4, 834–860. [CrossRef]).
24. Themeßl, M., Gobiet, A., Heinrich, G., 2012. Empirical statistical downscaling and error correction of regional climate models and its impact on the climate change signal. *Clim. Chang.* 112 (2), 449–468.
25. Fowler, H., Kilsby, C., 2007. Using regional climate model data to simulate historical and future river flows in northwest England. *Clim. Chang.* 80, 337–367.
26. Graham, L., Andréasson, J., Carlsson, B., 2007. Assessing climate change impacts on hydrology from an ensemble of regional climate models, model scales and linking methods—a case study on the Lule river basin. *Clim. Chang.* 81, 293–307.
27. Wilks, D., 1995. Statistical methods in atmospheric science. In: Volume 59 of International Geophysics Series. Academic Press, San Diego, London.
28. Wilcke, R., Mendlik, T., Gobiet, A., 2013. Multi-variable error-correction of regional climate models. *Clim. Chang.* 120 (4).
29. Wilcke, R., 2014. Evaluation of Multi-Variable Quantile Mapping on Regional Climate Models. ISBN 978–3–9503608-3-7. Wegener Center Verlag, Graz PhD thesis.
30. Themeßl, M., Gobiet, A., Leuprecht, A., 2011. Empirical statistical downscaling and error correction of daily precipitation from regional climate models. *Int. J. Climatol.* 31 (10), 1530 – 1544.

31. Gumbel, E., 1935. Les valeurs extrêmes des distributions statistiques. *Annales de l'Institut Henri Poincaré* 5 (2), 115–158.
32. Gil Lemos, Alvaro Semedo, Mikhail Dobrynin, Melisa Menendez, and Pedro M. A. Miranda, 2020. Bias-Corrected CMIP5-Derived Single-Forcing Future Wind-Wave Climate Projections toward the End of the Twenty-First Century. *Journal of Applied Meteorology and Climatology*. Volume 59: Issue 9, 1393–1414.